

Abstract

A ballasted railway track will be created for laboratory experimentation at NTNU from January to June 2023. It will be located in the laboratory owned by the Department of Civil and Environmental Engineering. The objective of this master's thesis is to construct the best possible functional 1:5 railway track from easily accessible material.

The scaled track will be approximately geometrically similar to Bane NOR's superstructure class d. However, distortions of physical properties are inevitable, and scaling laws must be used when interpreting test results. For this scaled model, establishing geometrical similarity as a scaling condition ensures partial similarity, and the results from validation testing are used to suggest a useful scaling function.

The scaled model is built using exclusively commercially available material. This decision makes the construction cost-effective and time-efficient, albeit compromising properties and similarities. The rails are made of a T-profile steel bar, and the sleepers are made from a square steel pipe. The fastening system comprises square washers, bolts, and coupling nuts integrated into the sleepers. The scaled ballast material is made of crushed rock from Vassfjellet, with a grading curve that parallels Bane NOR's requirements down-scaled by a factor of 1/5.

The components are assembled to the Wigaard track (TWT), a functional 1:5 scaled ballasted railway track. TWT is a 2.5-meter tangent track with adaptable properties and is manageable to build and use.

A rigid frame is constructed to span the model's width, and a jack, a loading cell, and a dial gauge are fastened to the frame. The setup measures TWT's vertical deflection under a 4.4 kN axle load on each rail. The foundation coefficient is estimated to be 0.0478 N/mm^3 . This estimation predicts and compares the vertical load results to theory.

The validation test revealed that TWT had more vertical deflection than the theory suggests and that sleeper distance had significantly less influence on vertical deflection than expected. However, the results are linear, making it possible to suggest a scaling function that improves the mathematical predictions. Various factors can cause weak load distribution on TWT.

TWT is the first iteration of a versatile representation of a full-scale ballasted railway. The long-term goal is to create an apparatus that can produce meaningful data in multiple new loading situations. Such a model would be a valuable asset to the academic community at NTNU and the railway research community nationwide.

Sammendrag

Det vil bli laget et funksjonelt skalert jernbanespor for laboratorieeksperimentering ved NTNU fra januar til juni 2023. Sporet vil bli plassert i laboratoriet til instituttet for bygg- og miljøteknikk. Målet med denne masteroppgaven er å konstruere det best mulige funksjonelle 1:5 skalerte jernbanespor ved hjelp av tilgjengelig materiale.

Det skalerte sporet vil være omtrent geometrisk lik Bane NORs overbygningsklasse d. Forvrengninger av fysiske egenskaper er likevel unngåelige, og skaleringslover må brukes ved tolkning av testresultater. For denne skalerte modellen oppnås delvis likhet ved å etablere geometrisk likhet som en betingelse, og resultatene fra valideringstesting brukes til å foreslå en anvendbar skaleringsfunksjon.

Den skalerte modellen bygges utelukkende med kommersielt tilgjengelig materiale. Denne beslutningen gjør konstruksjonen tid- og kostnadseffektiv, men kompromitterer egenskaper og likhet. Skinnene er laget av et T-profil stålbjelke og svillene er laget av et firkantet stålrør. Befestigelsen består av firkantede skiver, bolter og langmuttere som er innlemmet i svillene. Skivene klemmer skinnene fast til svillene. Det skalerte ballastmaterialet er laget av knust stein fra Vassfjellet. Kornfordelingskurven er parallell med Bane NORs krav, nedskalert med en faktor på 1/5.

Komponentene monteres til Wigaard-spor (TWT), et funksjonelt 1:5 skalert, ballastert jernbanespor. TWT er et 2,5 meter rettspor med justerbare egenskaper og er enkelt å bygge og bruke.

En stiv ramme bygges over modellens bredde, og en jekk, en lastcelle og et måleutrusting festes til rammen. Oppsettet brukes til å måle TWTs vertikale nedbøyning under en 4,4 kN aksellast på hver skinne. Ballastsifferet anslås å være $0,0478 \text{ N/mm}^3$. Dette anslaget forutsier og sammenligner resultatene fra den vertikale belastningstesten med teori.

Valideringstestene avslører at TWT hadde mer vertikal bøyning enn det teorien antyder, og at avstanden mellom svillene har betydelig mindre innflytelse på vertikal bøyning enn forventet. Imidlertid er resultatene lineære, noe som gjør det mulig å foreslå en skaleringsfunksjon som forbedrer de matematiske prediksjonene. Den svake lastfordelingen på TWT kan være forårsaket av ulike faktorer.

TWT er den første iterasjonen av en allsidig representasjon av et fullskala ballastert spor. Det langsiktige målet er å skape et apparat som kan produsere nyttige data i ulike nye lastsituasjoner. En slik modell vil være en verdifull ressurs for akademiske miljøer ved NTNU og jernbanefagmiljøet nasjonalt.

Preface

This thesis is the conclusion of my master's in Civil and Environmental Engineering at NTNU. The task was rewarding and fun, and I appreciated the opportunity to do practical laboratory work and draw conclusions from the data. An especially big thanks to Konnekt for covering financial costs and making research like this possible.

I have been supervised by Associate Professor Albert Lau from the Department of Civil and Environmental Engineering, NTNU. I thank him for his contributions, experience, and knowledge throughout the semester.

I would also like to thank Bent Lervik. His help with the laboratory work, providing equipment, suggesting and executing practical solutions, and guidance throughout the semester. Finally, thanks to Torbjørn Nerland and Tage Westrum for ordering and processing metal material.

The work in this thesis builds on the author's specialization project from the fall of 2022. It is not required to read the specialization project. Mostly it was a preparation consisting of a literature search and surveying design options. During the process, the thesis has been converted to an academic journal article which is included as the last appendix of the thesis. The article is 16 pages, where the main differences are the details in methodology and results and the number of pictures.



Trondheim, 2023
Are Wigaard

Contents

Abstract	i
Sammendrag	ii
Preface	iii
List of Figures	viii
List of Tables	ix
1. Introduction	1
1.1. Background and Motivation	1
1.2. Contribution, Research Objectives, and Research Questions	2
1.2.1. Contribution	2
1.2.2. Objectives	2
1.2.3. Scope	3
1.2.4. Research Questions	3
1.3. Structure of the Thesis	3
2. Theory	5
2.1. Scaling and Similitude	5
2.2. Ballasted Track	6
2.2.1. Components and Structure	6
2.3. Distorted Properties for the Down-Scaled Components	7
2.3.1. T-Profile Steel Bars as Down-Scaled Rails	7
2.3.2. Scaled Sleepers Made of a Square Steel Pipe	8
2.3.3. Fastening System	8
2.3.4. Scaled Ballast Material	9
2.4. Theoretical Relation Between Static Vertical Force and Vertical Deflection	9
2.4.1. Mathematical Formulas and Relevant Track Properties	10
2.4.2. Example of Calculated Theoretical Vertical Deflection	11
3. Material and Method	13
3.1. Material-Related Information and Material Pre-Processing for Individual Components	13
3.1.1. Rails	13
3.1.2. Sleepers	14
3.1.3. Fastening System	15
3.1.4. Ballast Material	16
3.2. Construction of the Scaled Model	19
3.3. Methods and Set-Up for Validation Testing	21
3.3.1. Vertical Load Set-Up	22
3.3.2. Determining Foundation Modulus for the Scaled Model	24
3.3.3. Static Vertical Load Test Method and Set-Up	25

Contents

4. Results and Discussions	29
4.1. The Wigaard Track (TWT)	29
4.2. Measuring the Foundation Coefficient	30
4.2.1. Expected Foundation Coefficient	30
4.2.2. Results from Foundation Coefficient Test	30
4.3. Static Vertical Load Test	31
4.3.1. Expected Results from Static Vertical Load Test	31
4.3.2. Results from Static Vertical Load Test	32
4.4. Suggested Scaling Function for Vertical Deflection	35
4.5. Discussions	36
4.5.1. Track Design and Static Vertical Load Test as Validation	36
4.5.2. Damaged Threads on the Loading Set-Up Causing Invalid Data	37
4.5.3. Properties of TWT	38
4.5.4. The Scaled Track's Loading Distribution and Characteristic Length	38
4.5.5. The Accuracy and Applicability of The Wigaard Function	38
4.5.6. Similarity and Representation of the Loading Situation	39
4.5.7. Range of Experiments	40
4.6. Lessons Learnt	40
5. Conclusion and Further Work	43
5.1. Conclusions	43
5.2. Further Work	44
A. Appendix	49
A.1. Grain Distribution of Vassfjellet's 8/11 and 4/8 Crushed Rock	49
A.2. The Thesis as an Academic Journal Article	52

List of Figures

2.1. Ballasted railway track's components	7
2.2. Scaled Rail Profile [mm]	7
2.3. Cross section of the scaled sleeper [mm]	8
3.1. Two 2.5 meter scaled rails	13
3.2. Scaled rails' cross-section	13
3.3. Placement of hexagonal holes	14
3.4. Filling scaled sleepers with concrete	14
3.5. Scaled sleepers filled with concrete	14
3.6. Square washers by the rail	15
3.7. Fastening system	15
3.8. Close-up of the fastening system	15
3.9. Improvised fastening solution for one damaged coupling nut	15
3.10. Distribution curve for scaled ballast material	17
3.11. Tangent ballast layer [mm]	18
3.12. Scaled tangent ballast layer [mm]	18
3.13. Acquiring crushed rock	18
3.14. Sieving machine and material	18
3.15. Weighing crushed rock	18
3.16. Floor space and rug	18
3.17. Shaping the ballast layer	19
3.18. Ensuring correct ballast height	19
3.19. Cross-section scaled ballast	19
3.20. Finished ballast layer	19
3.21. Aligned measuring tapes	20
3.22. Sleepers connected by rails	20
3.23. Structure lifted onto the ballast	20
3.24. Superstructure before tamping	20
3.25. Leveling the track with a spirit level	20
3.26. Sleepers halfway integrated in the ballast	20
3.27. Additional ballast material added	21
3.28. Sleepers fully integrated into the ballast	21
3.29. Fastening the rails once again	21
3.30. Finalized scaled model	21
3.31. Threaded rods fastened to the floor	22
3.32. Hollow profile metal posts for support	22
3.33. The frame spanning the scaled model	22
3.34. The rail as a beam, threaded rods, and fastening nuts	22
3.35. Load cell	23
3.36. Hydraulic jack	23
3.37. Dial gauge	23
3.38. Test position N	24
3.39. Test position C	24

List of Figures

3.40. Test position S	24
3.41. Hydraulic jack in contact with load cell	24
3.42. Load and measuring set-up for measurement of C-value	24
3.43. Screenshot from a recording of C-value measuring with plate 1	25
3.44. Screenshot from a recording of C-value measuring with plate 2	25
3.45. Sleeper distance 222 mm	26
3.46. Sleeper distance 153 mm	26
3.47. Sleeper distance 111 mm	26
3.48. Cylinder representing a wheelset	26
3.49. Platform to measure vertical deflection	26
3.50. Dial gauge placed on platform	27
3.51. Static vertical load set-up	27
3.52. Screenshot from a recording of a test	27
4.1. The Wigaard track, a functional 1:5 scaled ballasted railway track	29
4.2. Expected trends for vertical load tests	32
4.3. Data plot for $s=111$ mm	34
4.4. Data plot for $s=153$ mm	34
4.5. Data plot for $s=222$ mm	34
4.6. Data plot for every test	34
4.7. New expected results using suggested scaling function in the results plot	35
4.8. One damaged threaded rod	37
4.9. Another damaged threaded rod	37

List of Tables

2.1. Individual components of a ballasted railway track's superstructure	6
3.1. Requirements for ballast material	16
3.2. 1/5 linearly down-scaled requirements for ballast material	16
3.3. Scaled ballast material parameters and requirements	16
3.4. Formula for scaled ballast material	17
4.1. Price and commercial actor for each component	29
4.2. Normal values for foundation modulus on full-scale ballasted tracks	30
4.3. Test result from vertical resistance measuring of the scaled ballast layer	31
4.4. Relevant parameters of the scaled track for calculating deflection	32
4.5. The scaled track's theoretical response to the scaled loading situation	32
4.6. Results from all static vertical load tests	33
4.7. Comparison between the Wigaard track and a full-scale superstructure	39
A.1. Distribution in grams for each grain size interval for Vassfjellet 8/11	49
A.2. Distribution in percent of mass for each grain size interval for Vassfjellet 8/11	50
A.3. Distribution in grams for each grain size interval for Vassfjellet 4/8	51
A.4. Distribution in percent of mass for each grain size interval for Vassfjellet 4/8	52

1. Introduction

Two long-term goals significantly influence political transport infrastructure decision-making in Norway: The vision zero goal and the zero-growth goal [1]. The plans state that we shall have zero fatal injuries or deaths and that there shall be no increase in private car transports in major urban areas. Transportation by rail is safe and green, making it a natural political focus area. However, the rail network is limited outside metropolitan areas due to high investment costs caused by strict performance requirements. Large railway projects in Norway cost billions [2], but a lot can likely be optimized with more knowledge, experience, and competence with track design and construction [3]. Track design continuously evolves to improve safety, efficiency, and cost-effectiveness as technology improves, scientific discoveries are made, and transportation demand grows. Investing resources in scientific research ensures that the best possible effort is made when designing and maintaining railway tracks.

Experimentation on physical models is a practical method that can produce results and data unobtainable from calculation and theory alone. The method has enormous potential for scientific innovation, especially in civil engineering. However, full-scale model testing is demanding and dangerous. Furthermore, railway infrastructure is expensive and indispensable. A scaled model made to accurately represent a full-scaled track's behavior under stresses in a scaled system can be a viable apparatus for scientific innovation. The research described in this master's thesis aims to provide NTNU with an operable, scaled, ballasted railway track for functional laboratory experimentation. This paper describes relevant scaling theory, the construction process, material choices, and how the scaled track performs in a relevant loading situation. The scaled track is located in the laboratory owned by NTNU's Department of civil engineering, and the scale is chosen to be 1:5. This scale was chosen in order to fit the scaled model inside the department's existing snow lab, which opens the possibility for future experimentation in cold conditions. The timeframe is one semester, from January 2023 to June 2023.

1.1. Background and Motivation

Scaled ballasted railway track is a viable and versatile scaled apparatus for scientific research [4]. Nevertheless, they are rare and likely unutilized, and full-scale tests are expensive and often inaccessible. Consequently, trial-and-error experiments are uncommon in railway research, which limits possible innovation. An accurate representation of a railway track's behavior in a scaled system opens the range of physical experiments worth conducting. However, the scaling distorts the physical properties of the track, making a perfect representation impossible. This research is motivated by the pursuit of creating the best possible representation. This representation behaves similarly enough to produce meaningful data in various relevant loading situations. To succeed in creating this, one must consider a scaled system's physical limitations, dissimilarities, and uncertainties. Model testing will merely waste time and money if the experiment is too complex, and the scaled model is not expected to indicate realistic full-scale behavior [5]. Additionally, practical testing will have no advantages if theory alone can predict the results. These two criteria establish an explicit range for the usage of the scaled models.

1. Introduction

The small scale allows parameters to be changed quickly, good operability, and small space usage. Additionally, the monetary incentive to reduce the scale must not be underappreciated. The cost is reduced by cheaper construction, material, and, most importantly, reduction in loading magnitude [6]. The laboratory environment ensures known and carefully controlled conditions and isolates the effect of one parameter for each experiment.

The model will be kept simple due to price, operability, and the research's limited time-frame. The scaled model must be finished and validated before June 2023. Additionally, it should be replicable, affordable, and operable. Therefore, the scaled track will be built with common, commercially available materials without extensive processing. This decision will compromise the scaled track's performance and similarity. However, the advantage of low price, use of standard materials, and simplified assembling lowers the threshold for similar projects in the future, either recreations or improvements. More research on scaled models can eventually create a good enough representation to improve how railroads are designed.

1.2. Contribution, Research Objectives, and Research Questions

1.2.1. Contribution

The main contribution of this master's thesis is to provide NTNU with an operable and affordable apparatus for practical railway research and experience on the topic. The scaled model will consist of easily accessible material at a relatively low cost. Furthermore, if the scaled track performs well, other interested parties can be inspired to construct similar apparatuses for commercial or research purposes.

A literature search was conducted in the author's specialization project [7]. Previous research that uses scaled models tends to exclude the construction process. Therefore, this thesis will thoroughly describe the material choices and assembling process, encouraging further work to improve the scaled model constructed in this research.

Scaled models are rare in Norway. Much of the existing literature and models are found on the other side of the world, e.g., in Japan and China. The scarcity of scaled ballasted railway models and the often unsatisfactory description of design and construction is a knowledge gap this thesis attempts to fill.

1.2.2. Objectives

The goal of this master's thesis is to build the best possible scaled ballasted railway track model. The scale will be 1:5. For the scaled model, 'best possible' means the design, material, and assembling choices that make the model predict full-sized railway behaviors accurately for several scenarios. Construction of the scaled model will be done using commercially accessible material. The research is successful if the model is functional, operable, and produces reliable data. The primary objective can be concisely formulated:

Construct the best possible functional 1:5 railway model from easily accessible material

The secondary objective is to survey the similarity between the scaled model and full-sized railways. Conclusions on similarity will be made by validation testing on the assembled model.

1.2.3. Scope

The scaled model built in this research is approximately geometrically similar to a ballasted railway track's superstructure. Specifically, the scaled model is based on Bane NOR's superstructure class d [8]. However, the simplification and material choices make the scaled track differ from a perfectly downscaled superstructure class d. Thus, the scaled model represents a generic ballasted track. In the research following bullet points will be achieved:

- Construct a 1:5 scaled ballasted railway track. The track will be tangent and 2.5 meters long.
- The scaled model shall consist exclusively of rails, sleepers, a fastening system, and ballast resting on a concrete floor.
- Surface level theory concerning the relevant scaling effects.
- Detailed description of the material, construction, and validating process.
- Vertical load test to consider the scaled model's similarity and performance.

Only commercially available material will be used, and there will be no extensive processing of the prefabricated components. The validation on the scaled track will need to be more extensive to conclude how versatile the scaled model is. This research aims to take the first step in the validation process.

1.2.4. Research Questions

If answered, the research questions will illuminate the knowledge gap and fulfill the main objective.

- How does one build the best possible 1:5 scaled ballasted railway track with commercially accessible material?
- How similar to a full-sized railway track will the scaled track behave under static vertical load?
- What design compromises in the scaled track significantly impact its similarity to a full-scale track?

1.3. Structure of the Thesis

The thesis consists of five Chapters; 1-Introduction, 2-Theory, 3-Material and Methods, 4-Results, and 5-Conclusion and Further Work. The current Chapter, introduction, focuses on motivation, contribution, objective, and research questions. The research questions will be answered in Chapter 5. Chapter 2-4 provides necessary information and data to draw conclusions. Chapter 2, Theory, will be concise and relatively short, while greater focus and time is invested in Chapter 3, Materials and Method.

2. Theory

The theory discussed in this chapter is limited to an overview of scaling theory, the significant dissimilarities between the scaled model and a full-size track, and how relevant track forces affect a railway. The latter is to represent realistic stresses and forces in the scaled system. The scaled system aims to represent full-size properties and requirements for a ballasted railway track and uses properties of Bane NOR's superstructure class d as a reference. This class is chosen because it is a common superstructure on existing lines in the Norwegian rail network and a likely choice for future lines. Therefore, scaled dimensions and requirements of Bane NOR's superstructure class d are used in the scaled system, and its performance is used as a basis of comparison when analyzing similarity.

The scaled model will be designed approximately geometrically similar to superstructure class d. This down-scaling creates distortions. For example, a perfectly geometrically similar model in scale $1:n$ will have $1/n^2$ the surface area and $1/n^3$ the volume. The most significant distortions in properties relevant to this research's validation tests will be discussed. A full-scale loading situation will be analyzed at the end of the chapter. The loading situation is chosen as the weight of the nominal axle load of the relevant superstructure class. The scaling and railway theory will decide how to represent this load in the 1:5 scaled system. In other words, determine the magnitude of static vertical force used to validate the scaled model's similarity.

2.1. Scaling and Similitude

A scaled model represents a full-size structure reduced in size to perform experiments more efficiently. Representing a real-life structure as a scaled model will always lead to dissimilarities and changes. Rayleigh first discussed small-scale modeling interpreted through the principle of similitude and dimensional analysis in 1915 [9]. It has since been further reviewed and modified by Langhaar [5], amongst others. Laws of similitude must be used when interpreting test results [6]. However, finding a numerical coefficient through the principles of similarity is impossible. It will require deep calculation or experimentation [9]. For the scaled track constructed in this research, this means applying the results from validation tests to create a scaling function. The model will be geometrically similar to a ballasted railway track's superstructure, meaning lengths, shapes, and overall geometry will be equal in a 1:5 scale system. This approach is chosen to capitalize on the advantages of scale reduction on every component. Experimental validation of the scaled model will be conducted to develop a proper scaling function as a surrogate scaling law. A scaling law aims to accurately relate input and output parameters between the full-size track and the scaled model.

Reliable model studies require knowledge about the effect small scale has on the materials and the scaled structure. Generally, materials increase in strength as scale decreases due to the lower probability of flaws within smaller components [6, 10]. Furthermore, geometrically similar structures will be affected by gravity linear to their mass, which is downscaled cubically, making the lighter structure relatively less affected by its specific weight and thus stronger [9]. The first-mentioned effect must be emphasized, and the results from one scale cannot be directly compared to another [10].

2. Theory

The uncertainties associated with scaling are one reason scaled railway tracks are scarce. For an intricate structure like a railway superstructure, complete similitude is impossible. Instead, partial similarity is obtained by establishing geometrical similarity as a scaling condition. To correctly interpret data from scaled model testing, one must determine proper scaling factors, establish necessary conditions that relate the response behavior of the scaled system to the full-sized system, and understand how much the scale affects the accuracy of model behavior [11]. In this research, a full-scale track's theoretical vertical deflection under a static vertical load is the established condition for comparison with the scaled track's behavior.

2.2. Ballasted Track

This section has been taken from the author's specialization project and provides a brief explanation of the components of a ballasted railway track's superstructure and the components' functions for those who may not be familiar with it [7].

2.2.1. Components and Structure

Railway tracks undergo vertical, lateral, and longitudinal forces. These forces come from axle loads, guiding forces, and acceleration or thermal stress, respectively. The forces can be static or dynamic and often happen simultaneously. A good railway infrastructure must be resilient and rigid to withstand these loads. Each component of a ballasted track is designed to achieve this. The ballasted track consists of a superstructure and a substructure. Components and properties of the superstructure will be the focus of this section because that is what we aim to replicate. Within the superstructure, different components have different influences on the whole construction. Table 2.1 summarizes each component, its role, and its most common material, and Figure 2.1 illustrates the structure. Information is derived from Bane NOR's technical regulations [12]

Component:	Function:	Material:
Rails	Guide the wheelsets Work as a support beam Work as a return conductor Ensure an even and stable driving route Transfer the loads from rolling stock to the sleepers	Steel
Fastening system	Maintain structural gauge Resist bending and buckling of the rails Fasten the rails to the sleepers	Steel
Sleeper	Carry the rails and keep them in place Transfer loads from the rails to the ballast	Concrete
Ballast	Distribute loads evenly to the substructure Ensure friction with the sleepers Ensure internal friction and stability Drain water	Crushed rock

Table 2.1.: Individual components of a ballasted railway track's superstructure [7, 12, 13]

2.3. Distorted Properties for the Down-Scaled Components

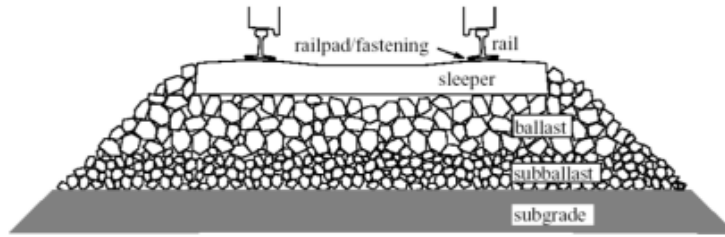


Figure 2.1.: Ballasted railway track's components
Illustration from [14]

2.3. Distorted Properties for the Down-Scaled Components

This section concerns each relevant scaled component's properties that differ far from 1/5 of the known corresponding full-size track's properties. The scaled rails loosely represent rail profile 60E1, and the scaled sleepers represent JBV60 concrete sleepers, which are valid full-scale choices for superstructure class d.

2.3.1. T-Profile Steel Bars as Down-Scaled Rails

T-profile steel bars will be used as rails on the scaled track. The height, width, and thickness are approximately 1/5 of the 60E1 rail profile. The scaled rail's bending stiffness is relatively weak compared to the 60E1 rail's. Using Equation 2.1, the scaled rail's moment of inertia is estimated to be **5.56 cm⁴**. The full-sized 60E1 profile's moment of inertia is **3038.3 cm⁴** [15], i.e., far greater than five times the scaled rail's moment of inertia. Bending stiffness is a critical parameter indicating the track's loading capacity and is the product of the moment of inertia and the material's elastic modulus. Both components are made of steel and have the same elastic modulus, \approx **210 GPa**. The difference in the moment of inertia causes a large difference in bending stiffness. Consider the moment of inertia over the scaled rail's lateral axis, I_x :

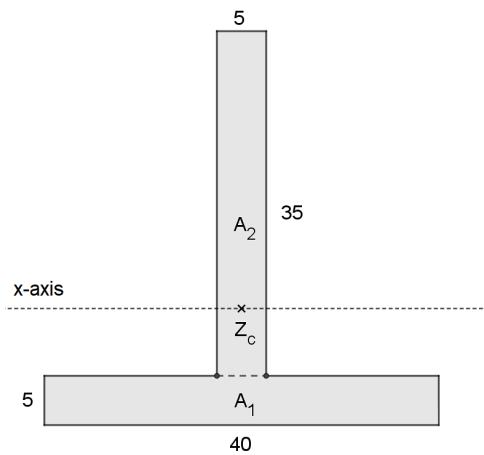


Figure 2.2.: Scaled Rail Profile [mm]
Illustration made with GeoGebra

- h_i = height of square i
- b_i = width of square i
- A_i = area of square i
- Z_c = Centroid of the cross-section
- e_i = Vertical distance from Z_c , to centroid of square i

With these defined parameters, the moment of inertia is given by equation 2.1

$$I_x = \sum_{i=1}^2 \left(\frac{1}{12} \cdot b_i h_i^3 + A_i \cdot e_i^2 \right) \quad (2.1)$$

Notice that the moment of inertia is down-scaled cubically with a cross section's height. Therefore, the down-scaling of height by a factor of 1/5 means 1/125 the bending stiffness.

2. Theory

This problem is inevitable when down-scaling. Additionally, the T-section geometry is sub-optimal compared to a rail with a railhead. There is less surface area far from the centroid, which drastically reduces e_2 , contributing squared to the total moment of inertia. This drastic reduction in bending stiffness must be accounted for when testing vertical loading capacity on the scaled model. Stresses applied to the scaled rails must never cause permanent deformations. Rail bending stiffness is crucial for obtaining a rigid, robust, high-quality railway track. It greatly influences the track's bearing capacity, rail bending stress, rail stiffness, and rail deflection [14].

2.3.2. Scaled Sleepers Made of a Square Steel Pipe

The sleepers are made of a hollow steel pipe with a cross-section of 40 mm · 60 mm and 3 mm thick walls. An illustration of the cross-section is included in Figure 2.3. The pipe's width and height are approximately 1/5 of the JBV60's width and height. The pipe will be cut into parts with a length of 480 mm, and this length is chosen to get the surface area that allows theoretical deflection and rail stress to be equal to a full-size railway simultaneously. The deflection and bending stress was verified using an Excel sheet based on the theory explored in Section 2.4. The sleeper length was optimized to achieve the best possible loading situation in the scaled system.

Because volume and weight are downscaled cubically, the scaled sleeper's weight will be drastically smaller than 1/5 of a full-sized sleeper. The relative difference in weight and material choice influences lateral resistance. Previous research found that the lateral resistance is expected to be 1/125 of a full-size sleeper [16, 17], and steel sleepers perform insufficient in dynamic lateral resistance[18]. The sleepers will be filled with concrete to increase the mass and geometrical similarity. The sleepers will have a mass of **4.5 kg**. Comparatively, one JBV60 sleeper weights **285 kg** [19].

The shape of the two sleepers is not geometrically similar either. The width of the JBV60 sleeper narrows toward the center to a width that would be 38 mm in scale. This geometry is quite different from the constant 60 mm shape of the scaled sleepers. Additionally, the cross-section of the full-scaled sleeper is a trapezoid shape, which the scaled sleeper does not resemble, possibly affecting its load distribution efficiency.

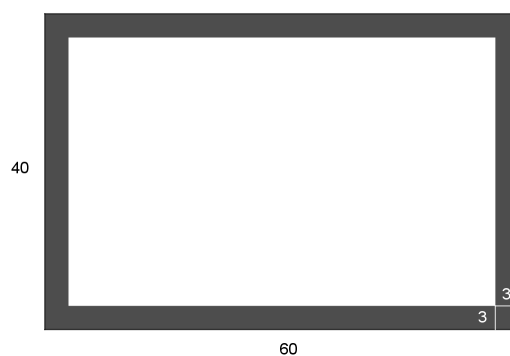


Figure 2.3.: Cross section of the scaled sleeper [mm]

2.3.3. Fastening System

The fastening system will be simplified and exclusively perform its primary function; holding the rail in place at constant track gauge. The standard track gauge is 1435 mm, which means a track gauge of 287 mm is chosen in the scaled system. The fastening system achieves this

2.4. Theoretical Relation Between Static Vertical Force and Vertical Deflection

by clamping the rail to the sleeper. Full-sized fastening systems perform a clamping force of 18 kN on each side of the rail $\pm 30\%$ [8]. For the scaled track, bolts and squared washers that can perform 1/5 of this force are chosen.

According to the principles of threaded fasteners and mechanics, the relationship between clamping force and applied torque for a bolted joint can be expressed as shown in Equation 2.2, where F is the clamping force, T is the applied torque, K is the coefficient of friction, and D is the nominal diameter of the bolt [20].

$$F = \frac{T}{D \cdot K} \quad (2.2)$$

The coefficient of friction is 0.2 for steel, which means the required torque is 5.7 Nm. The purchased bolts are by standard ISO4762, class 12.9, type MC6S and well suited for this torque based on advice from experienced engineers. Of course, this is only an estimation, and other factors can affect the accuracy of the calculation, such as the surface finish of the mating surfaces, the bolt's grade or strength, and the number of threads engaged in the joint. However, Bane NOR allows $\pm 30\%$, and an estimation is assumed to be sufficient. Further, the loads will be reduced by more than 1/5 when represented in the scaled system. The relative reduction entails that the simplified approach is expected to perform well enough. Insulation is also unnecessary because tests in this research will have no electric current.

2.3.4. Scaled Ballast Material

The goal is to produce scaled ballast material accurately representing a full-sized ballast layer. Previous research finds negligible differences in scaled grain's aspect ratio and concludes that scaled ballast material should have gradation parallel to the full-size material it represents [21, 22]. Therefore, the scaled model will use grain distribution parallel with Bane NOR's requirements [23, 24], down-scaled by 1/5. The grading curve is given in Section 3.1.4. The grading requirements on railway ballast are stricter than the margin of error on the available crushed rock in desired grain size range. Furthermore, the downscaled requirements do not necessarily match available standard sieving sizes. How this is overcome is also elaborated in Section 3.1.4.

Smaller grain sizes are statistically more robust because they are less likely to have internal flaws. If stresses on the large structure cause particles to break, the scaled ballast material is less compressible [22].

2.4. Theoretical Relation Between Static Vertical Force and Vertical Deflection

This research will conduct a static vertical loading experiment on the scaled model, where vertical deflection is measured. Vertical loading capacity is an essential measure of a track's quality and is chosen because the required set-up for applying a static vertical force is affordable and manageable. A criterion for the chosen validation test is that it must have a correct answer to strive for, and the relation between deflection and vertical load on a full-scale track can be calculated using theory. After obtaining the theoretical results, they can be compared to the measured results and used to evaluate the performance of the scaled track. This section aims to present this theory. Firstly, mathematical formulas used to calculate deflection, bending stress, and bending moment will be examined. Secondly, an example is explored to illustrate how these formulas are applied. The theory for full-scaled tracks will also be used to predict the scaled model's deflection before it is measured in the experiment.

2. Theory

The correct stress sizes to exert on the scaled model will be decided using theory. The static vertical load experiment corresponds to a static axle load. Modern full-scaled railway tracks have a maximum axle load between 16 and 25 tonnes [25]. For Bane NOR's superstructure class d, the nominal axle load is 22.5 tonnes. Theoretically, the load should be reduced proportionately to the square of the geometrical scale factor [6]. For the 1:5 scaled system, a 22.5 tonnes axle load should be represented by 8.8 kN static vertical force. Therefore, 4.4 kN on each rail will be the base when loading the scaled model.

2.4.1. Mathematical Formulas and Relevant Track Properties

Deflection, bending moment, and bending stress limit a railway's ability to handle large vertical loads. These parameters can be calculated for a full-sized track by treating the rails as a continuously supported beam. The theory is shown in Equation 2.3-2.5[14].

Deflection, y [m]:

$$y = \frac{Q}{2kL} \quad (2.3)$$

Bending moment, M [kNm]:

$$M = \frac{QL}{4} \quad (2.4)$$

Bending stress, σ [kN/mm²]:

$$\sigma = \frac{M}{W} \quad (2.5)$$

- Q = Wheel-load, [kN]
- k = track modulus, [N/m²]
- L = characteristic length, [m]
- W = second moment of area, [m³]

Track modulus, k , is the elastic support under the rails, depending on ballast, foundation, and sleepers. The support under the rails is:

$$k = \frac{C \cdot A_{rs}}{s} \quad (2.6)$$

- C = foundation coefficient, [N/m³]
- A_{sl} = area of the sleeper, [m²]
- s = sleeper distance, [m]

Characteristic length, L , is dependent on the rail profile and foundation and is calculated by:

$$L = \sqrt[4]{\frac{4EI}{k}} \quad (2.7)$$

- E = elastic modulus, [kN/m²]
- I = moment of inertia, [m⁴]

2.4. Theoretical Relation Between Static Vertical Force and Vertical Deflection

The second moment of inertia, W , is the moment of inertia, I divided by the vertical distance, z , from rail-foot to the cross-section's centroid. Equation 2.8 denotes the axis like Figure 2.2 and Bane NOR's technical regulations.

$$W = \frac{I_x}{z} \quad (2.8)$$

This theory is also utilized to predict the scaled track's vertical deflection. If the theory has a practical application on the scaled model, the scaled model is a good representation of a full-scale track under static vertical load. However, the parameters in the scaled system are distorted and not of comparable size to the full-scale parameters. The theory presented is developed for full-scaled systems and will likely be incorrect on a 1:5 scale. How much it differs will be analyzed to create a scaling function.

2.4.2. Example of Calculated Theoretical Vertical Deflection

The maximum allowed axle load for Bane NOR's superstructure class d is 22.5 tonnes, which means a Q-value of 110.36 kN. This loading situation is attempted to be represented in the scaled system to analyze the scaled track's behavior. Therefore, analyzing how a superstructure built with Bane NOR's class d theoretically behaves in the situation is relevant for comparison.

The needed parameters for superstructure class d are listed below:

- $C = 0.05 \text{ N/mm}^3$
- $A_{sl} = 0.624 \text{ m}^2$
- $s = 0.52 \text{ m}$

An Excel sheet was created where Equation 2.3-2.8, input parameters, calculated parameters, deflection, bending moment, and bending stress were related. The sheet was used as a tool for the entirety of this research. The example loading situation has the calculated parameters:

- $k = 57.4 \text{ N/mm}^2$
- $L = 0.817 \text{ m}$
- $W = 375 \text{ cm}^3$

Using a Q-value of 110.36 kN, we get these results for the theoretical loading situation:

- $M = 22.53 \text{ kNm}$
- $\sigma = 60.04 \text{ MPa}$
- $y = 1.18 \text{ mm}$

These three parameters are used to understand how the axle load affects the railway track and what limits the allowed axle load on different superstructure classes. The same Excel sheet, with the same theory, is used in the scaled system to predict vertical deflection, bending moment, and bending stress, with the scaled model's properties as input values. In this research, vertical deflection on the scaled model is the main focus and the only parameter to be measured in the validation test. Rail bending stress and moment will not be measured to

2. Theory

simplify the physical experiments and the cost of these. Some of the scaled model's properties are drastically different, e.g., the scaled rail's moment of inertia, and will likely affect the applicability of the theory.

The Excel sheet was then used to analyze the situation in the scaled system. The parameters that were not yet set in stone for the scaled system were tweaked to optimize the similarity between the scaled and full-sized loading situation. These parameters were sleeper distance, sleeper surface area, and load. The load of 4.4 kN proved to be a promising size to simultaneously achieve similar bending stress and vertical deflection while not distorting the sleeper's carrying surface or sleeper distance too far from their geometrical similarity condition. The example presented will be brought up in the discussion section of this thesis, together with a comparison between predicted and actual vertical deflection on the scaled model and the implications this has on similarity.

The Excel sheet also analyzed the maximum axle load to establish boundary values for the bending moment and bending stress. The bending moment will not be any problem, but the bending stress in the scaled system indicated that testing should not exceed the decided 4.4 kN value. If the load exceeded 4.4 kN, bending stress would be close to what the full-scaled system experiences under the maximum allowed axle load. Because 4.4 kN is the desired magnitude, there is no reason to push beyond this and risk permanent deformation on the scaled track.

3. Material and Method

The first part of this chapter will describe the material used in the scaled model and the methods used to assemble it. Next, the method and material used to conduct validation testing are described in detail. The validation tests will be the basis for the research's discussion. After reading this chapter, it should be possible to perfectly replicate the model and test methods done in this research. Many pictures from the laboratory work will be used to paint the correct picture of the process and the physical scaled model. Results and interpretation from the validation tests will be discussed in the last two Chapters.

3.1. Material-Related Information and Material Pre-Processing for Individual Components

This section describes the material used for each component of the scaled model. The material and design choices will be explained. Price will be brought up in Chapter 4.

3.1.1. Rails

T-profile steel bars were the only feasible option for the rails due to their commercial availability. A T-section with a height of 34.4 mm, a width of 30 mm, and a thickness of approximately 4 mm would be close to 1/5 of the 60E1 rail profile. Initially, a 35 mm · 35 mm T-section was preferred, but issues with steel distributors led to the purchase of 6 meters of 40 mm · 40 mm T-section with a thickness of 5 mm. The steel's quality is S235JR, and the moment of inertia is known. Although the chosen T-section is less similar in dimensions to a 35 mm · 35 mm T-section, it is more similar in bending stiffness to 1/5 of the 60E1 rail profile. To span the length of the chosen scaled track, the 6-meter T-section was cut into 2 · 2.5-meter lengths, shown in Figure 3.1-3.2.



Figure 3.1.: Two 2.5 meter scaled rails



Figure 3.2.: Scaled rails' cross-section

3. Material and Method

3.1.2. Sleepers

The scaled sleepers were made from a commercially purchased steel pipe with a 60 mm · 40 mm cross-section and 3 mm thickness. The steel is of quality S355J2H. A 1:5 scale replica of JBV 60 sleepers would be 520 mm · 44.5 mm · 60 mm. However, the pipe was cut into lengths of 480 mm to reduce the sleeper surface area. The resulting sleeper had a carrying surface area of 28,000 mm². According to the theory presented in Section 2.4, this value was a better fit to simultaneously achieve similar rail bending stress and vertical deflection on the scaled model as the full-size example given in Section 2.4.2. Four hexagonal holes were drilled in the hollow sleeper to accommodate the fastening system. Four threaded coupling nuts with a width of 17 mm, a height of 40 mm, and an internal diameter of 10 mm were placed in the custom holes. The holes were made at NTNU's laboratory. However, it could also be made by steel manufacturers, who often offer this for an additional fee. The placement of the holes, shown in Figure 3.3, was chosen to be symmetrically around each rail and ensure a track gauge of 287 mm, which is 1/5 · 1435 mm. The steel pipe sections were filled with concrete to provide additional mass and stability, as shown in Figure 3.4. The concrete poured around the bolts contributed to the fastening system's torque resistance. The resulting sleeper weighed 4.55 kg. The choice of a steel pipe and concrete filling provided a cost-effective and durable solution. The coupling nuts were integrated into the sleeper but stuck out slightly on one side. However, the protruding was less than the rail foot's thickness, thus making it possible to tightly fasten the rails on the side of the sleeper where the coupling nuts stuck out. The protruding also made for a better angle on the square washers used for fastening. Finished scaled sleepers are shown in Figure 3.5.



Figure 3.3.: Placement of hexagonal holes

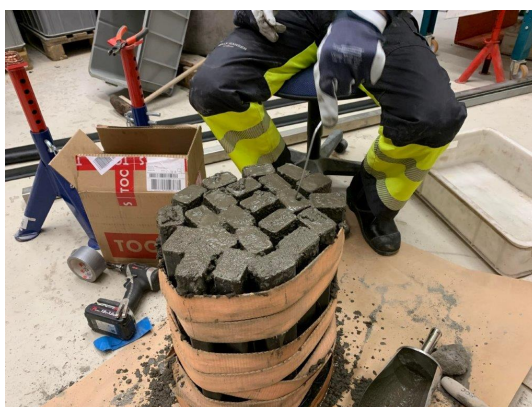


Figure 3.4.: Filling scaled sleepers with concrete



Figure 3.5.: Scaled sleepers filled with concrete

3.1. Material-Related Information and Material Pre-Processing for Individual Components

3.1.3. Fastening System

Square washers and bolts accompanying the coupling nuts made up the scaled fastening system. The square discs are 40 · 40 mm with a 12 mm diameter hole in the center, and the bolts have a diameter of 10 mm with an 8 mm head. The dimensions were chosen to perform a clamping force of 3.6 kN per bolt, as suggested in Section 2.3.3. In addition, bolts with an internal hexagon were chosen, making tightening easier in uneven situations.

Knowing the clamping force was not deemed critical to the results of this research as long as the primary function of the fastening system was achieved, which is to hold the rails in place and maintain the track gauge. The equipment needed to measure the clamping force was not conveniently available, and proceeding to assemble the model was deemed more beneficial for the research. As a result, measuring torque or clamping was not prioritized. The bolts were sufficiently fastened with a battery drill, ensuring every bolt was tightened equally.

One coupling nut was somehow damaged and could not be used as intended. The improvised solution was to jam a short threaded rod in the hole with a hammer and fasten the square disc with a standard nut, shown in Figure 3.9. It seemed to work sufficiently, but as a precautionary measure, this sleeper was not in use when not needed. Figure 3.6-3.8 shows how the fastening system held the rails.

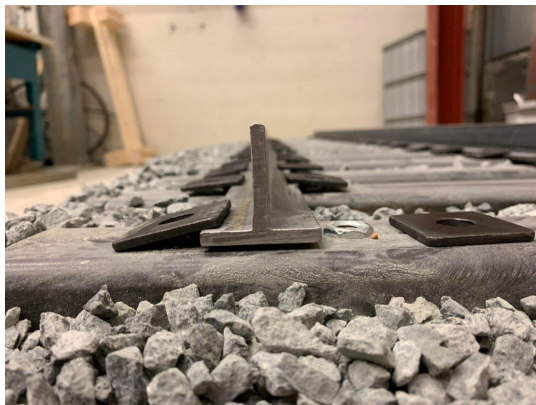


Figure 3.6.: Square washers by the rail

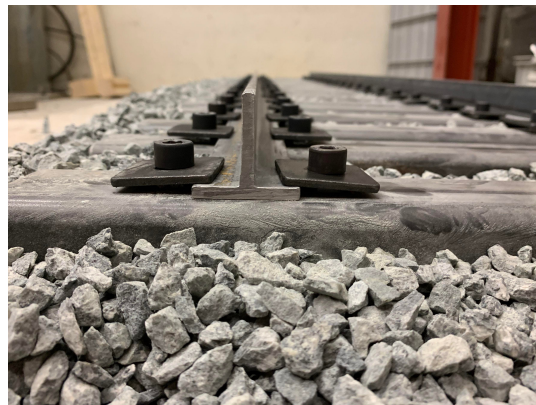


Figure 3.7.: Fastening system



Figure 3.8.: Close-up of the fastening system



Figure 3.9.: Improved fastening solution for one damaged coupling nut

3. Material and Method

3.1.4. Ballast Material

This section explains the production of scaled ballast material, which was the most comprehensive individual component of the scaled track. The scaled ballast represents a full-scale railway ballast. To achieve a good representation, requirements for the grain distribution will be parallel to Bane NOR's requirements, with a scaling factor of 1/5. At the same time, other relevant parameters such as Los Angeles-value, shape index, and Micro-Deval coefficient will be held to the same standards, which are listed in Table 3.3. Bane NOR's requirements for grain distribution are given in Table 3.1, and the parallel requirements, which the scaled model will be held to, are given in Table 3.2. The tables are extracted from the author's specialization project and Bane NOR's technical regulations. The quarry entrepreneur, Franzefoss, provides LA-value, MD-coefficient, and flakiness index. The shape index is not measured at the site for suitable grain sizes. Instead, it was measured by the author at the laboratory per standard NS-EN 933-4 [26].

Grain distribution full-sized ballast	
[mm]	% of total mass
80	100
63	95-99
50	55-99
40	25-75
31.5	1-25
22.4	0-3
31,5 - 63	≥ 50
Max fine grains (<0.5 mm)	0.6 % of total mass

Table 3.1.: Requirements for ballast material [7, 23, 24]

Grain distribution scaled ballast	
[mm]	% of total mass
16	100
12.6	95-99
10	55-99
8	25-75
6.3	1-25
4.48	0-3
6.3 - 12.6	≥ 50
Max fine grains (<0.1 mm)	0.6 % av total mass

Table 3.2.: 1/5 linearly down-scaled requirements for ballast material [7]

Property	Parameter	Requirement	Value
Resistance to fragmentation	Los-Angeles value	≤ 20	12
Resistance to wear	Micro-Deval coefficient	≤ 15	15
Grain shape	Flakiness index	No requirement	5-9
Grain shape	Shape index	≤ 20	7

Table 3.3.: Scaled ballast material parameters and requirements [23, 24]

Crushed stone was obtained from Vassfjellet quarry to produce the scaled ballast material. One pallet frame containing 8-11 mm and another 4-8 mm was needed. The material from Vassfjellet was sieved and analyzed to reveal its grain distribution. Results from this analysis are given in Appendix A.1. The scaled requirements for grain distribution differ from the available standard sieve sizes available to analyze grain distribution and produce sieved material. Therefore, the scaled requirements were plotted in an Excel sheet. Next, a grain distribution with available sieving sizes was customized to fit within the scaled maximum and minimum requirements. Finally, the plots were used as a visual tool to verify adequate grain distribution of the finished scaled ballast material, shown in Figure 3.10.

The analysis reveals that scaled ballast material cannot be produced by taking crushed

3.1. Material-Related Information and Material Pre-Processing for Individual Components

stone directly from the purchased pallet frames. Therefore, information from the sieve analyses was used to create a formula for a material with acceptable grain distribution. An effort was made to make the formula and the sieving process as simple as possible. Therefore, the formula used four components, which were 4-8 mm and 8-11 mm directly from Vassfjellet, as well as sieved 8-11 mm and sieved 6.3-8 mm. The sieved material is assumed to contain 100% of its mass within the given interval, while the un-sieved material is assumed to have grain distribution as discovered in the extensive sieving analysis, Appendix A.1. The formula utilizes as little sieved material as possible to reduce the workload. 20 kg of finished material was measured up and mixed at the time. Each partial weighing of each ingredient was rarely more than ± 0.01 kg from the intended partial sum. Thus, the finished material is undoubtedly within the scaled requirements. Table 3.4 shows the partial sums used when producing 20 kg of finished scaled ballast material. The total mass from each grain-size interval and the resulting grain distribution is also presented in Table 3.4. 680 kg of material was produced, approximately eight plastic cases, each containing 55 liters. This quantity provides 2.5 meters of rail with enough ballast material. Figure 3.10 shows the distribution curve of the material together with the predetermined requirements. The grain sizes in the distribution curve vary from the scaled requirements due to practicality and available sieve sizes. Max fine grains are the only parameter the scaled ballast material is not held to. Franzefoss ensured fine grains under 0.063 mm less than 1% and 1.3% of total mass for 8-11 mm and 4-8 mm respectively. However, the effort to wash and dry 680 kg of crushed rock was not deemed sensible time usage considering the dry conditions of the laboratory.

Box	Partial sum to 20 [kg]	Total mass [kg]	Resulting Grain distribution	
			[mm]	% of total mass
Vassfjellet's 8-11	3.54	120.4	16	100
Vassfjellet's 4-8	10.97	252.7	11.2	95
Sieved 8-11	18.05	240.7	8	42.3
Sieved 6.3-8	20	66.2	6.3	18.2
		$\Sigma 680$	5	4.2
			4	1.3

Table 3.4.: Formula for scaled ballast material

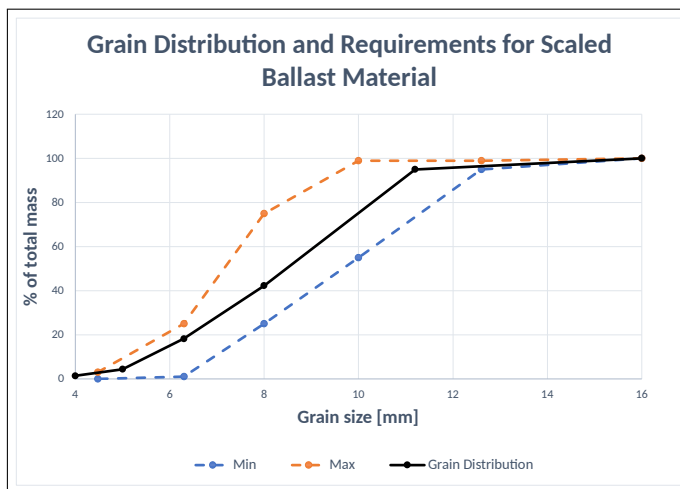


Figure 3.10.: Distribution curve for scaled ballast material

3. Material and Method

The layer's cross-section is linearly down-scaled with a factor of 1/5 from Bane NOR's standard ballast cross-section for a single tangent track. Figure 3.11 shows Bane NOR's full-size cross-section for the ballast layer, and Figure 3.12 shows corresponding dimensions for the scaled ballast layer. There is no substructure, and the ballast layer lies on a stiff surface. For this reason, a height of 800 mm is required on real railways [27], which corresponds with 160 mm in scale. Ballast height is measured from the floor to the top of the sleepers.

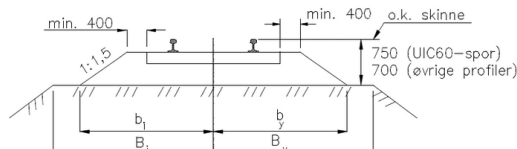


Figure 3.11.: Tangent ballast layer [mm]
[27]

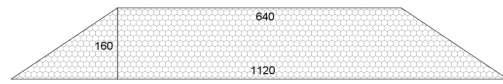


Figure 3.12.: Scaled tangent ballast layer
[mm]

The ballast was laid on a rug to increase friction because the concrete floor was slippery. The next step was to shape the ballast to the correct cross-section. Long, stiff metal bars resting on wooden supports at the correct height and markings on the rug were used as a frame of reference when creating the trapezoid shape of the cross-section. The ballast was then compacted and shaped with a shovel to dimensions given in Figure 3.12. Figure 3.13-3.20 are pictures from the process to illustrate.



Figure 3.13.: Acquiring crushed rock



Figure 3.14.: Sieving machine and material



Figure 3.15.: Weighing crushed rock



Figure 3.16.: Floor space and rug

3.2. Construction of the Scaled Model



Figure 3.17.: Shaping the ballast layer



Figure 3.18.: Ensuring correct ballast height



Figure 3.19.: Cross-section scaled ballast

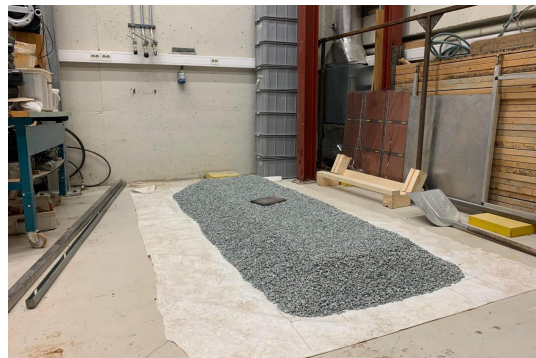


Figure 3.20.: Finished ballast layer

3.2. Construction of the Scaled Model

After the ballast layer was completed, the next step was to skim off approximately 20 mm of the top of the layer. The proceeding step was to align sleepers at correct and equal spacing. Longitudinal coordinates for each sleeper were defined using the sleeper distance as a reference. Two measuring tapes were then aligned parallel to each other from the first to the last sleeper, and the sleepers were placed at the correct millimeter value. The rails were then laid down on top of the sleepers. The slight protruding of the coupling nuts made it impossible not to get the correct track gauge. The rails were fastened, and the assembled track was lifted onto the ballast layer. Figure 3.21-3.23 illustrates the process.

The height of a ballast layer is measured from the subgrade to the top of the sleepers, i.e., the sleeper must be integrated into the ballast layer. The sleepers, rigidly connected by the rails, were jogged deeper into the ballast by pushing, stamping, and jiggling the structure back and forth. A spirit level was used to level the track, and the height was controlled easily by the frame visible in Figure 3.17 and 3.18. The rails were removed once the sleepers were level in both longitudinal and lateral directions and at the correct height. The sleepers were then buried in additional ballast material. This process served as the equivalent of full-scale tamping and is illustrated in Figure 3.24-3.30. Finally, the rails were fastened again, and the model was completed.

3. Material and Method



Figure 3.21.: Aligned measuring tapes



Figure 3.22.: Sleepers connected by rails

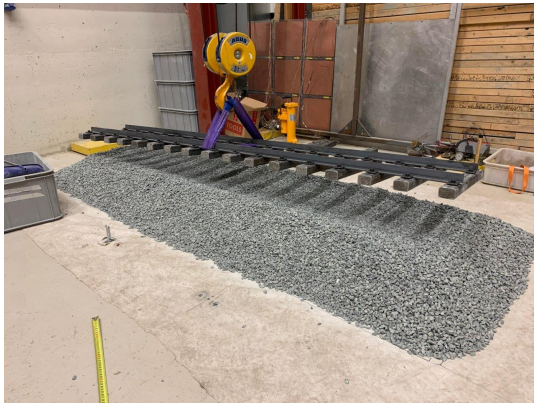


Figure 3.23.: Structure lifted onto the ballast

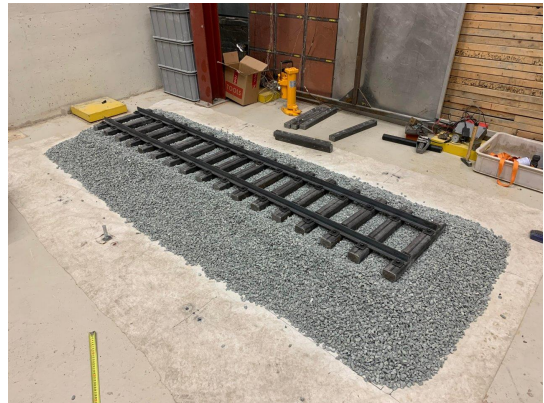


Figure 3.24.: Superstructure before tamping



Figure 3.25.: Leveling the track with a spirit level



Figure 3.26.: Sleepers halfway integrated in the ballast

3.3. Methods and Set-Up for Validation Testing



Figure 3.27.: Additional ballast material added



Figure 3.28.: Sleepers fully integrated into the ballast

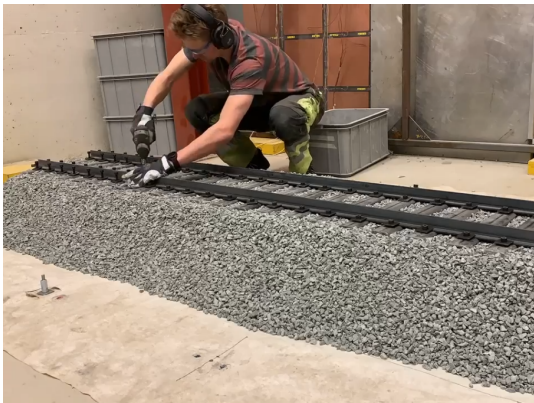


Figure 3.29.: Fastening the rails once again



Figure 3.30.: Finalized scaled model

3.3. Methods and Set-Up for Validation Testing

The model's behavior will be validated under static vertical load. The theory for full-scaled railway forces is utilized to predict vertical deflection. This test is chosen to check whether full-scale railway theory is applicable in the scaled system. If successful, the scaled model behaves similarly to that desired to replicate. To predict vertical deflection, the aforementioned Excel sheet served as a tool to calculate deflection quickly. The required input parameters are:

- Sleeper carrying area, A [m^2]
- Sleeper distance, s [m]
- Rail-profile moment of inertia, I [m^4]
- Rail elastic modulus, E [N/m^2]
- Vertical distance from rail-foot to the rail-profile centroid, e_i [m]
- Foundation coefficient, C [N/m^3]

3. Material and Method

The latter is the only unknown parameter and will be determined by experimentation before testing on the assembled model. It is satisfactory with a reasonable estimation, and six measurements are deemed sufficient. The testing will be executed because the vertical resistance in the scaled ballast layer cannot be guessed accurately. On real-life railways, the foundation coefficient is tested in the field similarly to the vertical load test that this research also conducts. However, because of the uncertainty surrounding the applicability of railway theory in the scaled system, a test that isolates the foundation coefficient is necessary. Such a test will provide an independent C-value estimation and reduce the sources of error when conducting the static vertical load test. The C-value measurement method is described in Section 3.3.2. The static vertical load test is conducted after a reasonable C-value is decided and is the main experiment in this research, described in Section 3.3.3. Both experiments use the same vertical load set-up and measuring equipment, elaborated in Section 3.3.1

3.3.1. Vertical Load Set-Up

As discussed in Section 2.4.2, it is desirable that the vertical load set-up is capable of performing up to 10 kN load onto the track. A frame was constructed to span the scaled model's lateral direction as shown in Figure 3.31-3.33. The frame had to be rigid enough not to have any measured displacement when subjected to forces of relevant magnitude. It is crucial for the integrity of the validation testing that all measured vertical displacement is on the scaled track. The available rigid beam was poetically enough a full-scale rail, shown in Figure 3.34. The beam was held against uplift by four nuts on four threaded rods fastened to the floor and supported by two hollow metal posts.



Figure 3.31.: Threaded rods fastened to the floor

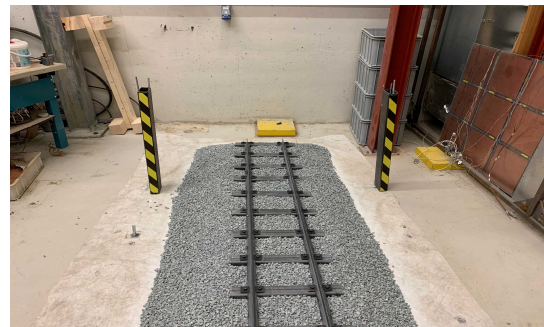


Figure 3.32.: Hollow profile metal posts for support

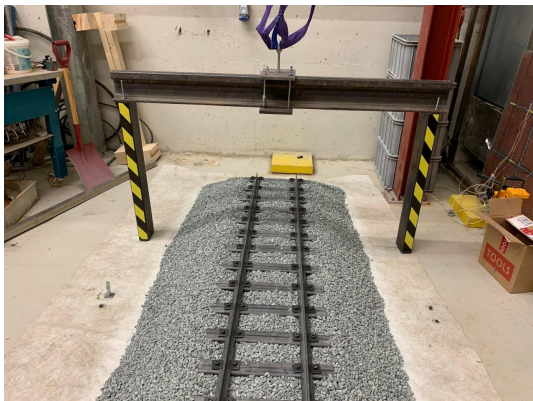


Figure 3.33.: The frame spanning the scaled model

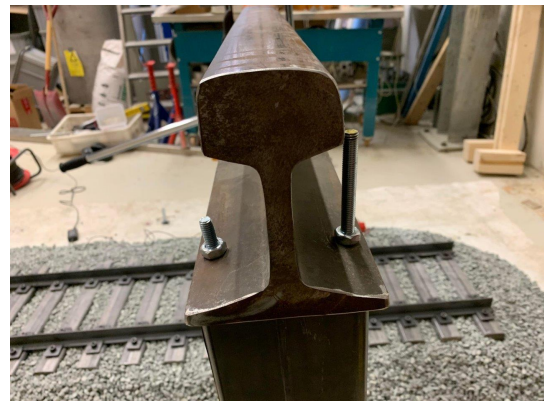


Figure 3.34.: The rail as a beam, threaded rods, and fastening nuts

3.3. Methods and Set-Up for Validation Testing

A manual hydraulic jack, capable of lifting 5 tonnes, and a load cell were placed between the frame and the scaled track. The load cell was calibrated and connected to a display. A dial gauge with 0.01 mm measuring accuracy was magnetically fastened to a stationary part of the jack. This way, it is possible to apply a vertical load on the track while also controlling and recording the numerical values of the force and vertical deflection. The recording was done with a smartphone, and the load was increased with one careful jack at a time, making it possible to discover the linearity of the load-deflection relationship. Force and deflection were plotted at three to four intervals. The average rate of increase on this plot is the desired parameter. The theory suggests that the plot should be linear throughout the entire loading process, as plastic deformation is undesirable. The load and measuring equipment are shown in Figure 3.35-3.37

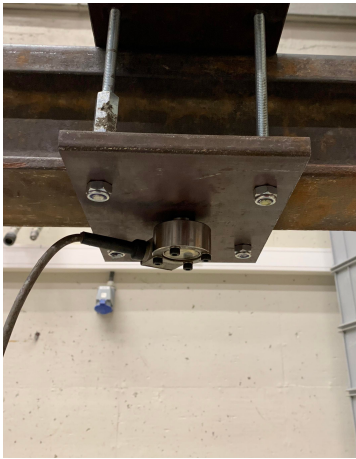


Figure 3.35.: Load cell

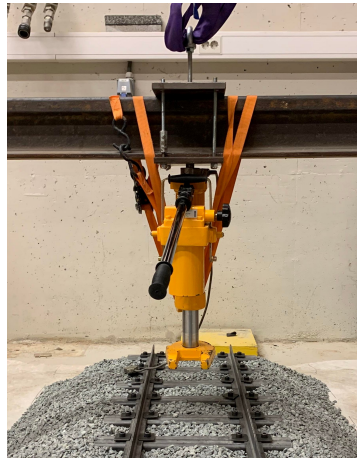


Figure 3.36.: Hydraulic jack



Figure 3.37.: Dial gauge

Creating a set-up capable of loading the track with the desired magnitude was the most challenging part of the construction and testing process. The frame components and measuring instruments are more expensive than the scaled model. This revelation is consistent with the theoretical proposition that the reduction of loading equipment represents the most crucial factor in cost savings associated with scaled structure research [6]. Creating more complicated loading situations can be challenging, time-consuming, and costly compared to the more straightforward static vertical load from one axle.

Three different testing positions were prepared. One testing position was at the longitudinal center of the scaled track, while two others were placed on the north and south sides, equally distant from the center and the track's ends. The positions were named N, C, and S, as shown in Figure 3.38-3.40. The distances from each testing position to the end of the track are shorter than its characteristic length. Consequently, tests from positions N and S should have the same deflection as those from position C, and if not, we have revealed fascinating information. Verifying this was the primary motivation for creating different test positions. Another advantage is getting C-values from different places and analyzing how evenly compacted the ballast layer is.

3. Material and Method

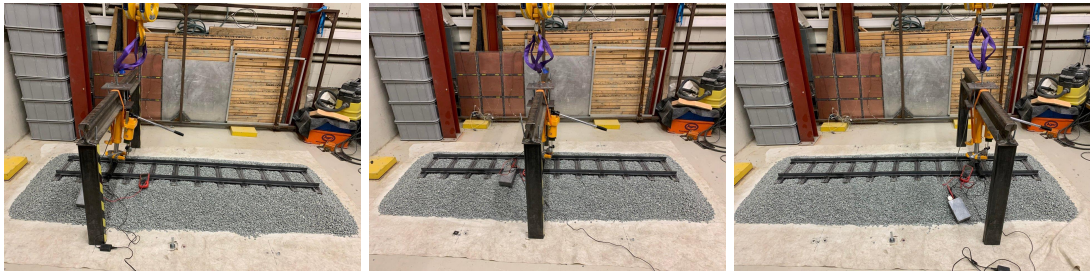


Figure 3.38.: Test position N Figure 3.39.: Test position C Figure 3.40.: Test position S

3.3.2. Determining Foundation Modulus for the Scaled Model

The foundation modulus will be measured with two unique steel plates as contact areas to the ballast layer. The plates are small to ensure the entire area is in contact with the ballast. The plates' load distribution is imperfect, but the experiment will reasonably estimate the C-value for later purposes. The motivation for two different rounds of testing with two different surface areas is to get twice the data and a better final estimation. Additionally, a potential difference between the results as a function of the surface area enables observation of the credibility of the measuring method. Ideally, the results should be independent of the plate's area, and no such trend should be discovered. Figure 3.41-3.44 are included to illustrate the method.

The C-value will be derived from the average rate of increase in a plot of the stress and corresponding deflection at three intervals. The dial gauge is accurate to 0.01 mm, providing the fortunate opportunity of not applying any oversized load to get precise readings. Too much load affects the ballast's compaction, which affects the parameter that's attempted to measure. The deflection will be kept under 1 mm, plotting the stress and deflection at three points before 1 mm deflection is reached. After the six individual tests are measured, the average C-value from each is the final estimation, which will be used as an input parameter for the theoretical vertical deflection of the scaled track. The components are assumed to have negligible deflection during the tests.



Figure 3.41.: Hydraulic jack in contact with load cell

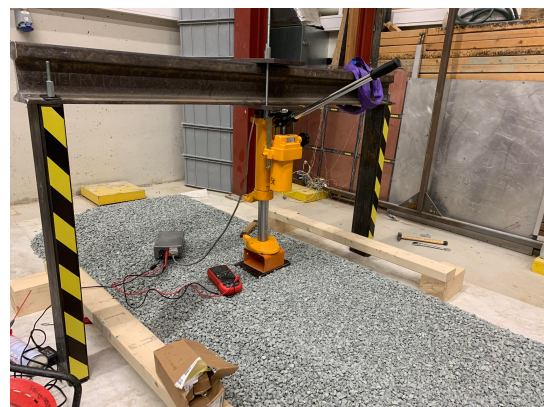


Figure 3.42.: Load and measuring set-up for measurement of C-value

3.3. Methods and Set-Up for Validation Testing



Figure 3.43.: Screenshot from a recording of C-value measuring with plate 1



Figure 3.44.: Screenshot from a recording of C-value measuring with plate 2

3.3.3. Static Vertical Load Test Method and Set-Up

For the vertical load validation testing, three different sleeper distances were tested, shown in Figure 3.45-3.47. The motivation to vary the sleeper distance was to get more data and to check whether this parameter has the same influence on vertical deflection as the theory suggests. Sleeper distances were decided by the number of sleepers available and the geometrical similarity to full-scale sleeper distance. The smallest sleeper distance tested was when all 23 sleepers were evenly spaced along the 2.5 meters of rails. Twenty-three sleepers gave a sleeper distance of 111 mm. The longest sleeper distance was twice this, 222 mm. The reason was to vary the sleeper distance enough to observe an apparent effect, and specifically, twice the distance was chosen due to the convenience of removing every other sleeper. The third sleeper distance tested was approximately in the middle, 153 mm. The model needed to be disassembled and reassembled for this middle sleeper distance.

3. Material and Method



Figure 3.45.: Sleeper distance 222 mm Figure 3.46.: Sleeper distance 153 mm Figure 3.47.: Sleeper distance 111 mm

The object in contact with the rails should represent a wheelset load, simplified in the mathematical formulas as a point load. The simplification means a cylindrical object spanning the track gauge is a good option, and the radius is unimportant. The cylinder used must be rigid enough not to have negligible vertical deflection in a loading situation. The cylinder chosen has a diameter of 45 mm and is made of steel, Figure 3.48. Based on the guidance of experienced laboratory engineers, it has been determined that the strength of the object is sufficient. A magnetic base was used to fasten the cylinder to the jack, which is ensured to be placed in the longitudinal center of the scaled track by fixed fastening on the frame. A small platform was fastened on the component perpendicular to the loading direction for deflection measurement shown in Figure 3.49. Figure 3.50-3.52 shows the test method in use.



Figure 3.48.: Cylinder representing a wheelset



Figure 3.49.: Platform to measure vertical deflection

3.3. Methods and Set-Up for Validation Testing



Figure 3.50.: Dial gauge placed on platform



Figure 3.51.: Static vertical load set-up

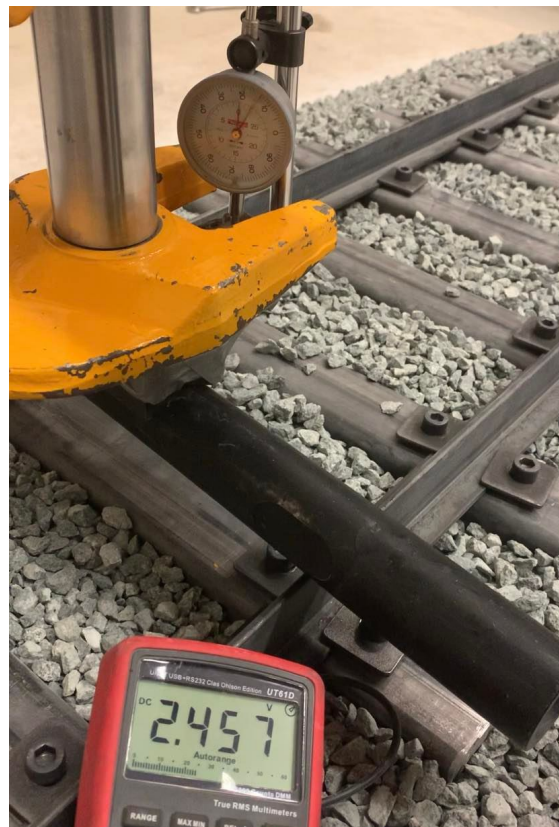


Figure 3.52.: Screenshot from a recording of a test

4. Results and Discussions

The chapter will present and discuss the results of the research. Data will primarily be presented as figures, graphs, or tables. The figures in this chapter are made in Excel.

4.1. The Wigaard Track (TWT)

The main result of the research is the finished, scaled model, named the Wigaard track, pictured in Figure 4.1. How viable it is as a functional apparatus for laboratory experimentation will be answered with the results from the validation tests and in Chapter 5. However, independently from those conclusions, the physical model is constructed and can be further validated, improved, and potentially used for innovative laboratory experimentation. The Wigaard track represents a tangent ballasted railway track on a scale of 1:5.

The price of each component and the rounded total cost of the scaled track is presented in Table 4.1. The cost was covered in its entirety by Konnekt. Transportation costs and the cost of material and equipment used in the validation testing are not included.

Role	Component	Amount needed	Commercial actor	Price
Rails	40·40 mm steel T-profile	1·6m	E.A. Smith	361 NOK
Sleepers	40·60 mm steel pipe	1·12m	E.A. Smith	1430 NOK
Fastening system	M12X40 square washers	100	TOOLS	538 NOK
	M10X35 bolts	100	TOOLS	366 NOK
	M10X40 Coupling nuts	100	TOOLS	769 NOK
Ballast material	Crushed rock 8/11 mm and 4/8 mm	≈ 800 liter	Franzefoss (Vassfjellet)	≈ 200 NOK
				Σ 3600 NOK

Table 4.1.: Price and commercial actor for each component



Figure 4.1.: The Wigaard track, a functional 1:5 scaled ballasted railway track

4.2. Measuring the Foundation Coefficient

The foundation coefficient, C , is the foundation and ballast layers' vertical resistance to deflection. It is interpreted as the support force performed per mm rail per mm deflection per mm width of a fictional infinitely long sleeper [28].

4.2.1. Expected Foundation Coefficient

The foundation coefficient is hard to guess beforehand, as many factors affect the C -value and uncertainty associated to the effect of scaling. On actual railways, the subgrade, temperature, maintenance, and ballast design influence the foundation coefficient. Typical parameters are presented in Table 4.2.

C-value [N/mm³]	Terrain
< 0.05	Soft sub-grade
0.05-0.15	Soft to firm clay
>0.3	Solid rock or concrete

Table 4.2.: Typical values for foundation modulus on full-scale ballasted tracks [29]

On concrete or exceptionally rigid sub-grades, the C -value can reach 0.5 N/mm^3 . The scaled model is placed on concrete, meaning if the C -value is $0.3\text{-}0.5 \text{ N/mm}^3$, the ballast layer is a good representation of a full-scale ballast track on concrete. However, as long as the results are within the ranges presented in table 4.2, the scaled model represents a normal vertical resistance, and the C -value is within an applicable range for the theoretical predictions of the upcoming vertical load test.

4.2.2. Results from Foundation Coefficient Test

The recording is done as described in Section 3.3.2. The deflection is noted at approximately 0 mm, 0.25 mm, 0.50 mm, and 0.75 mm, at values that got a clear, steady reading on both the load cell's display and the dial gauge. Results are presented in Table 4.3. Here, Δ denotes the parameter's value minus the initial value at the recording's beginning, which was zero for the deflection but always something for the force due to the hydraulic jack being strapped in place, hovering over the scaled model. The C -value is derived from each neighboring data point's rate of increase.

The results give foundation coefficient values within the expected range of full-sized ballasted tracks. The formulas for vertical deflection can be applied, and validation testing on the scaled track can proceed. However, the scaled model's C -value is significantly lower than usual on a stiff subgrade, showing the importance of this measurement for this research. The reason can be relatively weak compaction, the lack of large grains, the cubically reduced volume of the ballast layer, other scaling factors, or a combination of all mentioned. The standard deviation is somewhat large, making it difficult to conclude whether plate area or test position affected the measurements.

Without a predetermined C -value, any linear results would align with a custom C -value, which does not reveal how applicable the full-scale theory is in the scaled system, again justifying the independent measuring of the C -value. Unfortunately, the standard deviation of the measurements is high, and the C -value cannot be used as anything more than an estimation.

Test position	Plate area [mm^3]	Δ Force [kN]	Δ Deflection [mm]	C-value [N/mm^3]
NW	32000	0.491	0.28	0.0549
		1.110	0.65	0.0522
		1.583	0.91	0.0511
C	32000	0.273	0.25	0.0341
		0.575	0.47	0.0422
		0.918	0.78	0.0346
SE	32000	0.513	0.23	0.0697
		0.960	0.45	0.0635
		1.612	0.80	0.0582
NW	14400	0.0922	0.17	0.0377
		0.418	0.74	0.0397
		0.525	0.90	0.0464
C	14400	0.128	0.18	0.0492
		0.280	0.37	0.0556
		0.475	0.60	0.0589
SE	14400	0.128	0.19	0.0466
		0.302	0.54	0.0346
		0.394	0.75	0.0305
Standard deviation				0.0112
Average				0.0478

Table 4.3.: Test result from vertical resistance measuring of the scaled ballast layer

4.3. Static Vertical Load Test

The static vertical load test is this research's main effort in analyzing the scaled system's applicability as a functional testing apparatus. The analysis will be performed by comparing measured deflection with expected deflection calculated with known railway theory.

4.3.1. Expected Results from Static Vertical Load Test

Expected deflection will be calculated using theoretical formulas for rail deflection. Table 4.4 presents the parameters of the scaled track relevant to calculate expected bending stress, bending moment, and deflection.

The load chosen to represent a nominal axle load, 4.4 kN, is used in Excel to calculate the expected deflection, bending stress, and bending moment, presented in Table 4.5. When the expected deflection is estimated, a linear function from the origin establishes the expected results. Figure 4.2 shows the linear trend each sleeper distance is expected to approximate. results hopefully will approximate for all three sleeper distances.

With this plot and tables, there is established a basis for comparison with the measured data. The difference between measured and predicted data will be used to derive a scaling function, which adjusts expected results to fit the measured ones better and relate deflection in the scaled system to railway theory.

4. Results and Discussions

Parameter	Unit	Value		
I	cm ⁴	5.56		
E	N/mm ²	210000		
z	mm	11.83		
A _s	mm ²	28800		
C	N/mm ³	0.0478		
W	mm ³	4700		
s	mm	111	153	222
L	mm	248	268	295
k	N/mm ²	12.41	9.03	6.20

Table 4.4.: Relevant parameters of the scaled track for calculating deflection

Q ₀ = 4.4 kN								
s [mm]								
111	153	222	111	153	222	111	153	222
M [Nm]			σ [N/mm ²]			y [mm]		
272.43	295.01	323.98	57.97	62.77	68.93	0.7156	0.9087	1.2035

Table 4.5.: The scaled track's theoretical response to the scaled loading situation

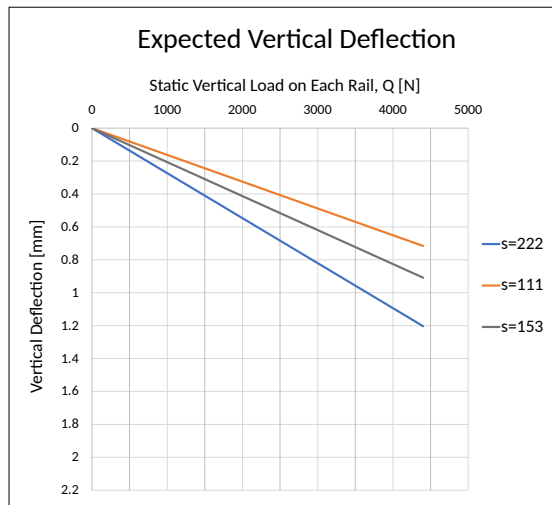


Figure 4.2.: Expected trends for vertical load tests

4.3.2. Results from Static Vertical Load Test

Table 4.6 presents all data points from the static vertical load tests. Figure 4.3 - 4.6 shows the same results plotted with the expected trend lines. Four points are plotted for every loading to check the data's linearity. The measured deflection is compared to the theoretical deflection at an equal vertical load, and the deviation is the difference between these divided by the measured deflection. Unfortunately, some data was invalid on the two last tests, the C and S test positions on sleeper distance 153 mm. The reason and implications will be discussed in Section 4.5.2. Half the results were valid, and together with the complete results of the two other sleeper distances, there is enough data to analyze and conclude.

4.3. Static Vertical Load Test

Sleeper distance 111 mm				
Position	Q [N]	y [mm]	Expected y [mm]	Deviation [%]
N	454.69	0.34	0.07	78.25
	1755.99	0.94	0.29	69.62
	2762.99	1.24	0.45	63.76
	4092.24	1.59	0.67	58.14
C	1599.52	0.78	0.26	66.65
	3235.34	1.13	0.53	53.43
	3975.99	1.35	0.65	52.10
	4456.68	1.51	0.72	52.00
S	235.93	0.35	0.04	89.04
	554.76	0.70	0.09	87.11
	2041.46	1.14	0.33	70.88
	4248.22	1.76	0.69	60.74

Sleeper distance 153 mm				
Position	Q [N]	y [mm]	Expected y [mm]	Deviation [%]
N	623.43	0.30	0.13	57.08
	1995.35	0.88	0.41	53.17
	2907.19	1.24	0.60	51.58
	3996.10	1.60	0.83	48.42
C	1198.29	0.52	0.25	52.41
	2272.49	0.91	0.47	48.43
	N/A	N/A		
	N/A	N/A		
S	N/A	N/A		
	N/A	N/A		
	N/A	N/A		
	N/A	N/A		

Sleeper distance 222 mm				
Position	Q [N]	y [mm]	Expected y [mm]	Deviation [%]
N	1681.43	0.32	0.46	-43.72
	3311.37	1.18	0.91	23.24
	3804.32	1.40	1.04	25.67
	4544.97	1.80	1.24	30.94
C	1552.92	0.72	0.42	41.01
	2599.06	1.22	0.71	41.73
	3653.73	1.55	1.00	35.52
	4649.45	1.97	1.27	35.45
S	604.30	0.50	0.17	66.94
	1961.02	0.98	0.54	45.27
	3888.19	1.79	1.06	40.59
	4717.14	2.03	1.29	36.44

Table 4.6.: Results from all static vertical load tests

4. Results and Discussions

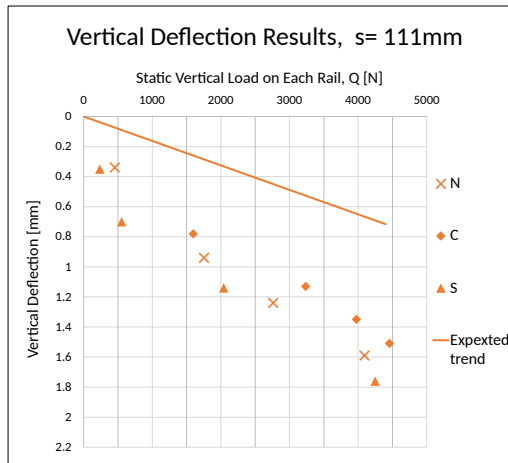


Figure 4.3.: Data plot for s=111 mm

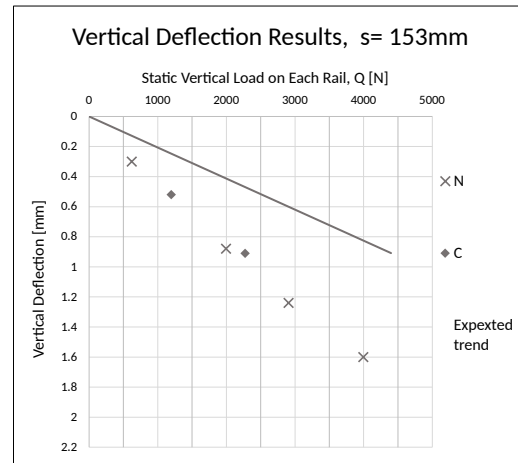


Figure 4.4.: Data plot for s=153 mm

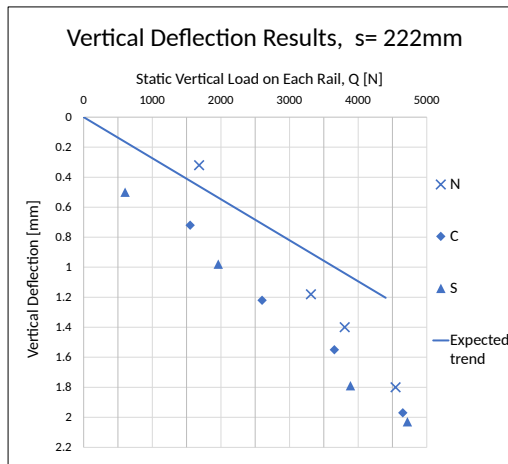


Figure 4.5.: Data plot for s=222 mm

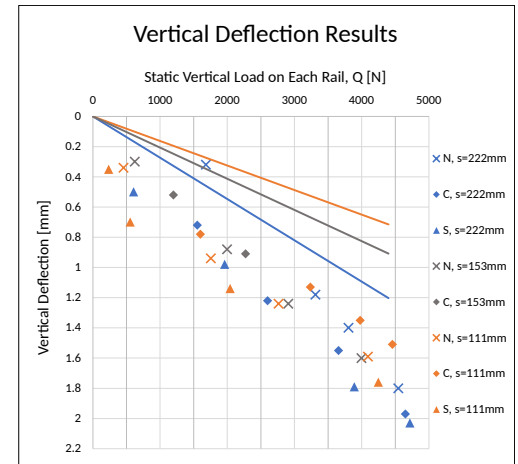


Figure 4.6.: Data plot for every test

All the measured data points in every test position and every sleeper distance, except one, show deflection values larger than expected. The greater the sleeper distance, the greater the deviation. In other words, the scaled track is relatively more prone to vertical deflection than a full-scale track, and the change of sleeper distance does not affect deflection as much as it does in full-scale theory.

The positive information to derive from these results is its linear trend. A data set's linearity can be measured with Pearson's correlation coefficient, r , as shown in Equation 4.1.

$$r = \frac{n(\sum x_i y_i) - \sum x_i \cdot \sum y_i}{\sqrt{(n \sum x_i^2 - (\sum x_i)^2) \cdot (n \sum y_i^2 - (\sum y_i)^2)}} \quad (4.1)$$

The results are close to linear, with a Pearson's correlation coefficient of 0.953, 0.997, and 0.948 for sleeper distances 111 mm, 153 mm, and 222 mm.

The best-matched linear trend line of every data plot has rates of increase that correspond to the effects of changing sleeper distance, respectively 0.3082 m/N, 0.4006 m/N, and 0.4007 m/N for the decreasing sleeper distance. The latter is only marginally different. Additionally, the middle sleeper distance lacks data, making it the most uncertain indication and difficult to conclude whether it is less resilient to vertical deflection than the shortest sleeper distance.

4.4. Suggested Scaling Function for Vertical Deflection

This result gives an improved mathematical formula for the relation between static vertical force and vertical deflection. The existing formula for full-scale tracks is used and expanded on with a function of sleeper distance. The function is exclusively applicable to TWT. The function is added to the existing formula and is named the Wigaard function, $W(s)$ - $W(s)$ takes sleeper distance as input in dimensionless meter value. Sleeper distance is a parameter in the existing formula, meaning it is possible to derive an entirely new mathematical formula for TWT with the same results. However, to recognize the changed mathematics, it will be added as a factor to existing theory. The Wigaard function is a product to be multiplied with the existing formula for deflection. This way, the difference and relations between the two are easily spotted and understood, and the function can be altered in the future if more data is obtained. The full-scale formula for deflection is repeated in Equation 4.2

$$y = \frac{Q}{2kL} \quad (4.2)$$

Notice that k depends on the foundation coefficient, C , which is 0.05 N/mm^3 for these conditions. Regression analysis on the deviation between measured and expected results is used to derive the Wigaard function, $W(s)$, in Equation 4.3. The Wigaard function is the best-fitted power function that ensures the logical consequence of changing sleeper distance and the lowest possible average deviation between measured and calculated results.

$$W(s) = 0.823 \cdot s^{-0.494} \quad (4.3)$$

Vertical deflection of the Wigaard track can be calculated with Equation 4.4

$$y = \frac{Q}{2kL} \cdot W(s) \quad (4.4)$$

$$y = \frac{Q}{2kL} \cdot 0.823 \cdot s^{-0.494}$$

This new mathematical formula for vertical deflection gives new trend lines on the results plot, which is shown in Figure 4.7

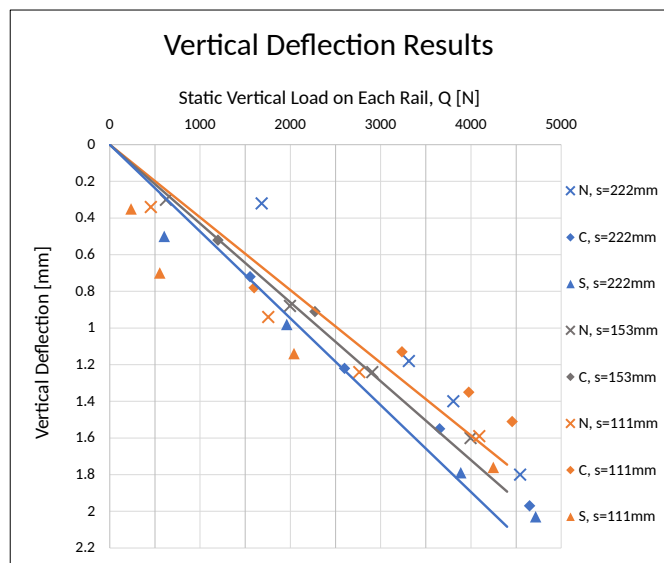


Figure 4.7.: New expected results using suggested scaling function in the results plot

4. Results and Discussions

The Wigaard function works best for the sleeper distance of 153 mm and must never be used for sleeper distances over 222 mm or under 111 mm. It gives a 19.03% average percent deviation for $s=111$ mm, -18.5 % for $s= 222$ mm, and only -0.36 % deviation for $s=153$ mm. Comparatively, the average deviation before implementing $W(s)$ was 66.81%, 51.85%, and 31.39% for sleeper distances 111mm, 153mm, and 222mm. The function is designed this way because bending stress and deflection for sleeper distances between 111 mm and 222 make for good representations of the loading situation in Section 2.4.2. Additionally, the two extreme sleeper distances are distorted beyond reasonable representation. The longest sleeper distance is almost as long as its characteristic length, meaning the force is barely shared by more than one sleeper. The shortest sleeper distance has only 51 mm of spacing between the ends of the width of each sleeper. The spacing becomes relatively short compared to a full-scale track due to the slight distortion of sleeper width and the lack of narrowing width toward the center of the sleeper.

The number $W(s)$ is dimensionless and can be calculated as a scaling coefficient if the sleeper distance is constant. For example, the sleeper distance that is closest to 1/5 of 600 mm using the whole track and a whole number of sleepers is 128 mm. A scaling coefficient of 2.28 can be used instead of the formula for this constant sleeper distance.

4.5. Discussions

This section will discuss the finished model's properties, similitude, realism, and overall performance. The choice of validation test and sleeper distances will be discussed and justified, and the incidence that caused invalid data on one-and-a-half tests and its implications on the research will be discussed. Then, the test results will be compared to the expected results from theoretical calculation, and the deviation will be the basis for our eventual conclusion.

4.5.1. Track Design and Static Vertical Load Test as Validation

The test is chosen for four crucial reasons:

- The set-up provides accurate and controlled loading conditions.
- Vertical deflection reveals the scaled track's loading capacity and indicates overall quality and rigidity.
- The test and measuring equipment are simple, manageable, safe, and reliable.
- The measured results can be compared to theoretical values for vertical deflection.

The sleeper distance was the parameter chosen to change for different tests because it was the quickest way to test tracks with different parameters. The shortest sleeper distance was chosen when all 23 sleepers were in use. The longest was double this due to the convenience of removing every other sleeper. These two distances were also deemed the shortest and longest sleeper distance worth testing. Any sleeper distance shorter than 111 mm would have presented difficulties surrounding integrating the sleepers into the ballast layer. The maximal sleeper distance worth testing was 222 mm because any longer sleeper distance would result in an almost equal or greater theoretical characteristic length. The characteristic length is the length of the rail affected by deflection, and if this does not span more than one sleeper, the sleepers do not perform their purpose in distributing load to the ballast layer.

The track was chosen to be 2.5 meters for two reasons. First, it had to be long enough to conduct tests at multiple positions where no test was closer to the edge of the track than the

characteristic length, representing a representation of a tangent track going on forever. The track was no longer because one 12-meter steel pipe provided just enough sleepers for 2.5 meters, given a sleeper distance 1/5 of Bane NOR's superstructure class d, which means a significant saving in material expenses and a track that was long enough for the purposes of this research. The test results showed no indication that the characteristic length ever exceeds theoretical estimations.

4.5.2. Damaged Threads on the Loading Set-Up Causing Invalid Data

The validation testing took an abrupt end when the nuts holding the loading frame in place slipped. Two threaded rods were worn out, Figure 4.8-4.9, and the frame no longer had a negligible vertical deflection. The incident happened spontaneously at the end of the second last planned test. The last test was also conducted, but it was apparent throughout the testing that the frame was no longer rigid, and when plotting the data, it became even more apparent that the data was useless. Either the set-up was less capable than first presumed, or the author tightened the nuts unevenly. The incident made a loud enough sound to be heard on the recordings, thus making it possible to plot data up to when the nut slipped and distinguish valid and invalid data.

The valid data obtained from the affected sleeper distance followed the expected deflection. Therefore, it was deemed unnecessary to finish testing. The relatively little data missing would be more effort to obtain than it was worth. Considering the data we got followed the expected pattern, i.e., it showed that the vertical deflection was greater than the theory suggested. The data also showed that the trend line's rate of increase was between the longest and the shortest sleeper distance's trend lines'. The average percentage deviation from theoretical deflection was also between the large and small sleeper distances. The hypothetical values of the tests not conducted were not expected to provide any information beyond what was possible to derive from the valid data. Thus the decision was made to proceed with the next step in the research.

The data from tests with a sleeper distance of 153 mm is nevertheless more uncertain than the other. The trend line's rate of increase and the Pearson correlation coefficient are estimations and would naturally have benefited from more data.

Suppose the vertical validation is to be repeated. In that case, the threaded rods should be upgraded to a larger diameter, and the nuts should be longer coupling nuts to better distribute the forces on more threads. The new data set should be used for improved regression analysis, i.e., revisit and update the scaling function.



Figure 4.8.: One damaged threaded rod



Figure 4.9.: Another damaged threaded rod

4. Results and Discussions

4.5.3. Properties of TWT

TWT has several adjustable features, which means it can be altered to best fit future research. Two of the most manageable parameters to change include ballast height and sleeper distance. One can also shorten sleepers to get a smaller surface area supporting the rails. Reduction of sleeper area increases deflection more than bending stress, making it possible to simultaneously get both parameters equal to a full-size railway under any given axle load. Naturally, there is no way back to the original sleeper length, so caution is advised. Changing the sleeper distance is the most convenient way to tweak the track's properties. Once a loading set-up is completed, experimenting with the scaled system is quick and easy. These conveniences are essential to capitalize on the benefits of the reduced scale. The track is 2.5 meters long and takes up approximately 3 m² of floor space when assembled. The ballast can fit on one pallet with three pallet frames and is about 700 kg, which makes up most of the total model's weight. The transportation and set-up equipment are excluded from the cost estimation because the equipment used was already available at NTNU's laboratory, and the set-up and transportation will be different for each research purpose. However, the costs of the loading set-up must not be forgotten when planning similar research.

4.5.4. The Scaled Track's Loading Distribution and Characteristic Length

The results show that sleeper distance has a less prominent effect on deflection than it has in theory. This difference between theory and measurements is indisputable and significant for all three sleeper distances. The reason why more sleepers do not increase the track resistance to vertical deflection can be poor load distribution. In other words, the characteristic length, i.e., the length of rail affected by vertical deflection, is shorter than the theory suggests. Consequently, the load is distributed over fewer sleepers, and the resulting maximal deflection is relatively higher.

In theory, the longest sleeper distance had a characteristic length spanning only 1.33 sleepers. If the characteristic lengths are shorter than the theory suggests, it might not span multiple sleepers, and the sleepers will not distribute the load as they should. In such a scenario, the conditions of sleeper distance 222 mm would drastically differ from the two others, explaining why this trend line's rate of increase was distinct from the two others. Additionally, the trend line's rate of increase for the two other sleeper distances was indistinguishable because the actual characteristic length spanned approximately the same number of sleepers.

Another possible explanation for the relatively weak load distribution of the scaled track is that the sleepers do not distribute the load as efficiently as a full-scaled sleeper. In this scenario, the scaled sleeper's shape, material, or relative reduction in surface area due to scaling impedes its ability to perform well as a load distributor.

A third factor that can explain the observed effect is the relatively weak bending stiffness of the rails. If the rails do not distribute the load as well as its full-scale counterpart, the vertical deflection will be relatively high. Even though the scaled rail's bending stiffness is accounted for in the theoretical calculations, the distortion relative to every other crucial parameter is considerable and can affect the applicability of the mathematical formulas.

4.5.5. The Accuracy and Applicability of The Wigaard Function

The results from the three different sleeper distances are visually similar on the result plots, and one can interpret from the scaling function that the new expected relation between vertical deflection and force is less dependent on sleeper distance. Furthermore, it is possible to derive a scaling function where the sleeper distance is irrelevant or has the opposite ef-

fect, i.e., greater sleeper distance decreases the expected vertical deflection. The regression analysis used the condition that greater sleeper distance results in more significant vertical deflection. This condition made some regression attempts invalid. For example, to weigh outlying data less, use another power, or use a different type of function.

The method used to arrive at the Wigaard function was to minimize inaccuracies on values around 153 mm and allow the extremes to have some. Consequently, the method resulted in a positive deviation from theory for small sleeper distances and a negative for longer ones. In other words, even when applying a scaling function that reduces the effect of sleeper distance on the vertical deflection, the actual effect is still smaller than the new theory suggests. The limited amount of data used to derive the function is the reason it is called a function and not a scaling law. Even if all tests were completed, it would be premature to address it as a law, and more tests should be carried out before it is statistically sound.

4.5.6. Similarity and Representation of the Loading Situation

The scaled model behaves linearly under static vertical load, as it should, but it does not follow the mathematical theory applied to real-life railways. The results and derived scaling function may only be applied to this specific model, with sleeper distances between 111 mm and 222 mm.

Table 4.7 presents the loading situation desired to replicate throughout the validation testing, i.e., one static nominal axle load on Bane NOR's superstructure class d. The table also compares the Wigaard track's current best representation of this loading situation. The sleeper distance is the closest possible to 1/5 of 600 mm using the whole track and a whole number of sleepers. The distance is between 111 mm and 222 mm, meaning the scaling function should provide an accurate theoretical deflection.

The scaled system's set-up for representing a nominal axle load		
Number of Sleepers	Sleeper Distance [mm]	Scaling Coefficient
20	128	2.27
Full-scale loading situation		
Q [kN]	y [mm]	σ [MPa]
110.36	1.18	60.04
Scaled system's representation		
Q [kN]	y [mm]	σ [MPa]
4.4	1.81	60.1

Table 4.7.: Comparison between the Wigaard track and a full-scale superstructure

The sleeper distance is approximately 1/5 of 600 mm, a standard full-scale sleeper distance, achieving geometrical similarity. The static load of each rail in the scaled system is 1/25 of the full-scaled system, as predicted in Chapter 2. The theoretical bending stress is virtually the same. However, it depends on the characteristic length, which is suspected to not coincide with the theory for the scaled system. The deflection is significantly higher on the scaled track, but it is impossible to reduce it significantly for the scaled track as it is currently designed. The bending moment is not of comparable magnitude, as shown in Section 4.3.1, and is therefore not listed in the table.

4. Results and Discussions

4.5.7. Range of Experiments

As mentioned in Section 1.1, experimentation on the scaled model must be simple enough to produce reliable data and complicated enough to be impossible to predict from theory alone. This section suggests some opportunities for innovation based on previous research and the static vertical load test results. However, it should not be read as a definitive list. Future research on the scaled model is encouraged to be creative.

- Surveying different sleeper designs' lateral resistance.
- Researching effects of cold weather inside NTNU's snow laboratory.
- Bearing capacity and vertical resistance on various ballast shapes and heights.
- Loading distribution on different scaled rail profiles.

Conclusions and potential innovation can only be made by someone familiar with the results of this research and the basic theory of scaling [5].

4.6. Lessons Learnt

The experiences learned throughout the research are shared below to be learned from:

- A considerable challenge at the beginning of this research was NTNU's new ordering system. A happenstance had it that NTNU had just introduced a brand new system for ordering construction materials when this research began. Precautions were made to avoid spending much time waiting for the material. The candidate had meetings with involved NTNU employees discussing what to buy several weeks before the official start of the master's thesis. An attempt was made to order every component at the beginning of the semester. However, because no one had any experience with the new system, several weeks passed after the start without the arrival of construction materials. Getting started on construction was also a deciding factor for only using commercially available materials. The decision was correct, as any longer time spent waiting on materials would likely result in delayed thesis submission.
- Another challenge for the research was coordinating the help from different laboratory engineers, all with other full-time commitments. Any project involving multiple actors is doomed to spend considerable time in communication, coordination, and planning. However, because this project depended on the help of NTNU employees with tight schedules, some time was spent waiting for materials processing or equipment. It is difficult to suggest a solution in hindsight because the laboratory engineers had essential competence, and the author needed help performing some tasks, e.g., drilling hexagonal holes in the scaled sleepers.
- The research's approach to laboratory work was to do everything simply so that it could not be done wrong. This philosophy influenced the research's decision-making, construction, purchases, load set-up, and focus areas. Undoubtedly it helped to keep the sources of error to a bare minimum. Unfortunately, however, it limited what was possible to achieve. Consequently, this research has only taken a small step in the quest for a reliable laboratory apparatus. However, it is a safe and vital first step that is manageable for the research's competence and time.

- Complex loading situations would be exponentially more challenging to represent in scale and increase uncertainties. The load experiment performed in this research was one of the simplest imaginable, and yet it was the most comprehensive and expensive part of the research. This experience leads the author to believe that more complex and dynamic loading situations would increase the difficulty beyond the ability of a master's candidate. Additionally, the uncertainties of scaling effects would exponentially increase as more distorted parameters are relevant for theoretical calculations.
- The C-value measurements had a high standard deviation. The standard deviation implies that one cannot be sure that the value of 0.0478 N/mm^2 is a good representation of the conditions along the scaled track. However, a wrong C-value will still indicate the correct effect of sleeper distance change and linearity of the data plots. Therefore, the main conclusions of this research are based on these two observations.
- Even though the testing was manageable to conduct alone, it would be easier with help. Naturally, the assembling and testing would be quicker, but also the readings on the validation testing could be easier to interpret. It is unlikely that the data points plotted have compromised validity. However, if one person focused solely on carefully applying load and another focused solely on recording, it could have produced more data points where a steady reading could be derived.
- Scaling laws and a deep understanding of similitude are outside the scope of this thesis. However, it is highly relevant to interpret results from future usage of the scaled track. These areas were not studied in depth to prioritize the physical construction and testing of the scaled model.
- The decision to shorten sleeper length to reduce area and increase theoretical vertical deflection more than theoretical bending stress was perhaps a mistake. Calculation beforehand revealed that the vertical deflection of the scaled track was lower than the full-scale track at similar bending stresses. However, after testing and applying the scaling function, the opposite problem was discovered. It is impossible to know if longer sleeper distances would have solved this problem, but one could have tried experiments on the longer sleepers first, then cut it shorter if necessary.

5. Conclusion and Further Work

This chapter aims to conclude the research. The conclusions are drawn with the results produced, and the experience gained is used to suggest further work on the scaled track. Further work should improve TWT as a functional representation of a full-scaled ballasted railway track.

5.1. Conclusions

This section presents concise answers to the research question and an assessment of the objective based on the results and discussions. The conclusion of this research is:

- The best possible 1:5 scaled ballasted railway track is built over several iterations. It is necessary to research available materials and purchase those with dimensions closest to 1/5 of a full-scale track. The next step is to assemble and test the behavior of the scaled track. Afterward, the behavior of the scaled track is compared with the desired behavior, any distortions that cause dissimilarities are identified, and improvements are suggested. This process is repeated until the track is expected to produce meaningful results that cannot be predicted solely through theory.
- The scaled track has relatively high vertical deflection under static vertical load. However, a full-scale nominal axle load situation can be accurately represented in the scaled system with a sleeper distance of 128 mm and a load down-scaled by 1/25. Furthermore, a scaling function can be used to predict vertical deflection on the track. For a sleeper distance of 128 mm, vertical deflection can be calculated with the full-scale mathematical formula multiplied with a numerical coefficient of 2.27.
- The scaled track does not distribute vertical force as well as a full-scale track. Amongst the relevant track properties for this research, the bending stiffness of the scaled rail is distorted most in the scaling. The distortion is caused by both the reduction in scale and the compromise made for commercial availability and likely has a profound effect on the rail's ability to distribute loads.

The objective of the research is to construct the best possible scaled track with commercially available material. The model constructed was much cheaper than anticipated and manageable to build, store, and conduct simple tests on for one person. There are better imaginable scaled representations of a ballasted railway track than this attempt. However, it is the best possible first iteration of a functional scaled ballasted railway track, considering the author's limited time frame, previous experience, and the commercial availability condition. The research is the first step in creating a versatile representation of a full-scale ballasted railway track that can produce meaningful data in multiple new loading situations. This ultimate goal is still further down the road and will require more iterations of the model, cooperation, and sharing of experiences.

5.2. Further Work

Further work on the Wigaard track is the only way to produce a multi-purpose scaled model for laboratory experimentation that can be used for railway technology innovation. Such a model would be a valuable asset to the academic community at NTNU and the railway research community nationwide. This section presents thoughts on improvements, new validation tests, and ambitions for the future of the scaled track. The list below should be read as suggestions. Future researchers must be imaginative and choose research suitable for their motivation and competence. The author will not participate in further research on the scaled model but will naturally be of guidance if needed.

Replacing the scaled rails: The vertical load test should only be repeated with significant changes on the scaled track. However, the test is quick to conduct, and all the work in designing the load set-up and equipment calibration is already done, and more data can be produced for relatively little effort. One exciting possibility is to change the scaled rails and do the same vertical loading experiment. A scaled rail profile resembling a full-scale rail, i.e., having a railhead, could improve the scaled model's load distribution, which is currently one of its most prominent flaws. A railhead would increase the bending stiffness of the scaled rail and, consequently, its qualities as a bearing beam.

Replacing the scaled sleepers: The scaled sleepers' lateral resistance could be validated and replaced if necessary. This research has not prioritized validating the sleeper's lateral resistance because it does not influence static vertical load significantly. However, it is one of the most critical factors to achieve a rigid and durable track for situations with lateral and longitudinal forces. If the sleepers are to be replaced, it would also be interesting to perform the static vertical load test again to verify if the new sleepers affected the scaled track's load distribution. New sleepers can also be made the same way, with increased length and sleeper surface area. A larger sleeper area will theoretically decrease the vertical deflection. Consequently, improve one of the flaws of the current scaled design.

Dynamic load validation test: The scaled track can be validated under dynamic loads. One such validation test was suggested in the author's specialization project [7], which would verify the scaled track's natural resonance frequency. The validation test could be performed with an excitation hammer and a laser-based vibrometer. The hammer would deliver dynamic loads, the vibrometer would measure the track's acceleration, and the frequency and receptance would be plotted.

Research the model inside the snow laboratory: Cold weather research in NTNU's snow laboratory is a natural ambition for the scaled track. The scale was explicitly chosen to make this possible, and the potential for valuable findings is immense for countries increasingly exposed to harsh weather like Norway. Research in the snow laboratory involving humidity or frost heave requires ballast washing.

Bibliography

- [1] Det kongelige samferdselsdepartement. Nasjonal transportplan 2022-2033, cited 2023 jan 25. Available at <https://www.regjeringen.no/contentassets/fab417af0b8e4b5694591450f7dc6969/no/pdfs/stm202020210020000dddpdfs.pdf>. Norwegian.
- [2] P. Qvale. Dette er de ti største jernbaneprosjektene i norge. *Teknisk ukeblad*, 2015. Available at <https://www.tu.no/artikler/dette-er-de-ti-storste-jernbaneprosjektene-i-norge/222395/>. Norwegian.
- [3] Ø. Nordli and W. Riaz. Kostet 36 milliarder – fungerte ni dager – stengt hele januar. *Aftenposten*, 2022. Available at <https://www.aftenposten.no/norge/i/AP7xmE/kostet-36-milliarder-fungerte-ni-dager-stengt-hele-januar>. Norwegian.
- [4] Vahid Najafi Moghaddam Gilani, Mohammad Habibzadeh, Seyed Mohsen Hosseinian, and Reza Salehfard. A review of railway track laboratory tests with various scales for better decision-making about more efficient apparatus using topsis analysis. *Advances in Civil Engineering*, 2022:9374808, 2022.
- [5] H.L. Langhaar. *Dimensional Analysis and Theory of Models*. John Wiley & Sons, 1951.
- [6] Harry G Harris. *Structural modeling and experimental techniques*. CRC Press, Boca Raton, Fla, 2nd ed. edition, 1999.
- [7] A. Wigaard. Surveying design and scaling strategy of a 1:5 scaled ballasted railway track for functional laboratory experimentation, des 2022. Specialization project, not available online.
- [8] BaneNOR. Teknisk regelverk/overbygning/prosjektering/sporkonstruksjoner/, [updated 2022; cited 2022 okt 18]. Available at <https://trv.banenor.no/wiki/Overbygning/Prosjektering/Sporkonstruksjoner>. Norwegian.
- [9] Rayleigh. The principle of similitude. *Nature*, 95(2368):66–68, 1915.
- [10] Aksana Jihad Mohammed, Naseer Babangida Muazu, Baba Shehu Waziri, and Taghadosi Ahmad. Models and size effects: A review. *IOSR Journal of Mechanical and Civil Engineering*, 12:54–59, 2015.
- [11] Shadi Balawi, Owais Shahid, and Mohammad Al Mulla. Similitude and scaling laws - static and dynamic behaviour beams and plates. *Procedia Engineering*, 114:330–337, 2015.
- [12] BaneNOR. Teknisk regelverk, [updated 2022; cited 2022 Okt 07]. Available at <https://trv.banenor.no/wiki/Forside>. Norwegian.
- [13] Jernbanekompetanse.no. Sporets komponenter, cited 2022 okt 20. Available at https://www.jernbanekompetanse.no/wiki/Sporets_komponenter. Norwegian.

Bibliography

- [14] A. Lau. *Compendium TBA4225 Railway Engineering, Basic course*. NTNU, 2022.
- [15] BaneNOR. Teknisk regelverk/overbygning/prosjektering/sporkonstruksjoner/vedlegg/skinneprofiler/60e1, [updated 2022; cited 2022 okt 11]. Available at <https://trv.banenor.no/wiki/Overbygning/Prosjektering/Sporkonstruksjoner/Vedlegg/Skinneprofiler#60E1>. Norwegian.
- [16] Yohei Koike, Takahisa Nakamura, Kimitoshi Hayano, and Yoshitsugu Momoya. Numerical method for evaluating the lateral resistance of sleepers in ballasted tracks. *Soils and Foundations*, 54(3):502–514, 2014.
- [17] H Tomita, Kimitoshi Hayano, and P Anh. Effects of model scale on lateral resistance characteristic of sleepers in railway ballasted tracks. In *Bearing Capacity of Roads, Railways and Airfields*, pages 2047–2054, 06 2017.
- [18] Morteza Esmaeili, Saeed Majidi-Parast, and Ahmad Hosseini. Comparison of dynamic lateral resistance of railway concrete, wooden and steel sleepers subjected to impact loading. *Road Materials and Pavement Design*, pages 1–28, 05 2018.
- [19] BaneNOR. Teknisk regelverk/overbygning/prosjektering/sporkonstruksjoner/vedlegg/sviller/spennbetongsviller/jbv60, [updated 2022; cited 2022 Okt 18]. Available at https://trv.banenor.no/wiki/Overbygning/Prosjektering/Sporkonstruksjoner/Vedlegg/Sviller#SPENNBETONGSVILLE_JBV_60. Norwegian.
- [20] James A. Speck. *Fastening, Joining and Assembly Handbook*. McGraw-Hill Education, 2005.
- [21] Adam F Sevi. *Physical modeling of railroad ballast using the parallel gradation scaling technique within the cyclical triaxial framework*. Missouri University of Science and Technology, 2008.
- [22] Louis Le Pen, William Powrie, Antonis Zervos, Sharif Ahmed, and Sinthuja Aingaran. Dependence of shape on particle size for a crushed rock railway ballast. *Granular Matter*, 15, 12 2013.
- [23] BaneNOR. Tekniske spesifikasjoner/overbygning/ballast, [updated 2015; cited 2022 Okt 22]. Available at <https://trv.banenor.no/ts/Overbygning/Ballast>. Norwegian.
- [24] European committee for standardization. Aggregates for railway ballast. NS-EN 13450, 2002.
- [25] BaneNOR. Teknisk regelverk/wiki/tabelltillatt hastighet og maksimal aksellast for overbygningsklasser, [updated 2022; cited 2023 Jan 30]. Available at https://trv.banenor.no/wiki/TABELL:Tillatt_hastighet_og_maksimal_aksellast_for_overbygningsklasser. Norwegian.
- [26] European committee for standardization. Geotechnical investigation and testing - Laboratory testing of soil - Part 4: Determination of particle size distribution. NS-EN 933-4, 2008.
- [27] BaneNOR. Teknisk regelverk/overbygning/prosjektering/ballast, [updated 2022; cited 2022 okt 22]. Available at

<https://trv.banenor.no/wiki/Overbygning/Prosjektering/Ballast>.
Norwegian.

[28] BaneNOR. Teknisk regelverk/wiki/definisjon:ballastsiffer, cited 2023 May 07]. Available at <https://trv.banenor.no/wiki/Definisjon:Ballastsiffe>. Norwegian.

[29] Jernbanekompetanse.no. Ballastsifferet, cited 2023 mar29 22. Available at <https://www.jernbanekompetanse.no/wiki/Dimensjoneringsmetoder#Ballastsifferet>.

A. Appendix

A.1. Grain Distribution of Vassfjellet's 8/11 and 4/8 Crushed Rock

Vassfjellet's 8/11 mm

Sample mass [g]	Distribution [g]					
	>16 [mm]	11.2-16 [mm]	8-11.2 [mm]	6.3-8 [mm]	4-6.3 [mm]	<4
1672	0	350	1117	165	29	8
1687	0	357	1150	157	21	4
1869	0	515	1183	142	21	5
1532	0	439	957	120	16	2
2167	0	506	1486	156	19	3
2057	0	502	1355	148	28	10
1998	0	566	1270	133	22	3
1864	0	468	1215	150	22	3
1985	0	572	1273	126	16	4
1756	0	525	1094	120	13	3
1910	0	679	1132	86	10	1
1879	0	537	1215	111	13	1
1920	0	605	1179	110	11	9
1996	0	537	1315	117	17	4
1953	0	477	1335	117	17	4
1971	0	523	1346	81	9	1
1582	0	375	1028	150	24	3
1887	0	465	1241	158	16	2
1655	0	531	963	143	15	7
1721	0	533	1035	138	12	6
1781	0	543	1073	147	15	2
1757	0	501	1098	142	23	1
1618	0	458	1017	120	36	5
1046	0	343	574	88	38	3
1734	0	653	903	166	24	1
1830	0	530	1122	158	22	2
1801	0	521	1134	120	27	2
1637	0	490	999	134	19	2
1796	0	636	1023	103	19	5

Table A.1.: Distribution in grams for each grain size interval for Vassfjellet 8/11

A. Appendix

	Distribution [%]					
	>16 [mm]	11.2-16 [mm]	8-11.2 [mm]	6.3-8 [mm]	4-6.3 [mm]	<4 [mm]
Average	0.00	28.41	62.83	7.401	1.15	0.21
Relative standard deviation	0.00	0.14	0.064	0.20	0.53	0.65
Sample mass [g]						
1672	0.00	20.93	66.81	9.87	1.73	0.48
1687	0.00	21.16	68.17	9.31	1.24	0.24
1869	0.00	27.55	63.30	7.60	1.12	0.27
1532	0.00	28.66	62.47	7.83	1.04	0.13
2167	0.00	23.35	68.57	7.20	0.88	0.14
2057	0.00	24.40	65.87	7.19	1.36	0.49
1998	0.00	28.33	63.56	6.66	1.10	0.15
1864	0.00	25.11	65.18	8.05	1.18	0.16
1985	0.00	28.82	64.13	6.35	0.81	0.20
1756	0.00	29.90	62.30	6.83	0.74	0.17
1910	0.00	35.55	59.27	4.50	0.52	0.05
1879	0.00	28.58	64.66	5.91	0.69	0.05
1920	0.00	31.51	61.41	5.73	0.57	0.47
1996	0.00	26.90	65.88	5.86	0.85	0.20
1953	0.00	24.42	68.36	5.99	0.87	0.20
1971	0.00	26.53	68.29	4.11	0.46	0.05
1582	0.00	23.70	64.98	9.48	1.52	0.19
1887	0.00	24.64	65.77	8.37	0.85	0.11
1655	0.00	32.08	58.19	8.64	0.91	0.42
1721	0.00	30.97	60.14	8.02	0.70	0.35
1781	0.00	30.49	60.25	8.25	0.84	0.11
1757	0.00	28.51	62.49	8.08	1.31	0.06
1618	0.00	28.31	62.86	7.42	2.22	0.31
1046	0.00	32.79	54.88	8.41	3.63	0.29
1734	0.00	37.66	52.08	9.57	1.38	0.06
1830	0.00	28.96	61.31	8.63	1.20	0.11
1801	0.00	28.93	62.97	6.66	1.50	0.11
1637	0.00	29.93	61.03	8.19	1.16	0.12
1796	0.00	35.41	56.96	5.73	1.06	0.28

Table A.2.: Distribution in percent of mass for each grain size interval for Vassfjellet 8/11

A.1. Grain Distribution of Vassfjellet's 8/11 and 4/8 Crushed Rock

Vassfjellet's 4/8 mm

Sample mass [g]	Distribution [g]					
	>11.2 [mm]	8-11.2 [mm]	6.3-8 [mm]	5-6.3 [mm]	4-5 [mm]	<4
1832	0.00	266.00	657.00	692.00	152.00	65.00
1983	0.00	286.00	788.00	651.00	158.00	95.00
1680	0.00	314.00	615.00	591.00	116.00	40.00
1778	0.00	258.00	598.00	734.00	147.00	40.00
1612	0.00	366.00	607.00	534.00	98.00	29.00
1666	0.00	311.00	568.00	618.00	110.00	56.00
1615	0.00	250.00	523.00	652.00	125.00	60.00
1576	0.00	275.00	560.00	594.00	103.00	44.00
1821	0.00	340.00	605.00	688.00	139.00	49.00
1746	0.00	259.00	582.00	669.00	142.00	84.00
1684	0.00	293.00	650.00	605.00	98.00	32.00
1568	0.00	262.00	516.00	587.00	115.00	84.00
1842	0.00	256.00	630.00	719.00	163.00	69.00
1670	0.00	280.00	572.00	631.00	139.00	47.00
1596	0.00	243.00	560.00	554.00	143.00	99.00
1656	0.00	287.00	593.00	653.00	92.00	32.00
1594	0.00	231.00	568.00	592.00	145.00	61.00
1756	0.00	223.00	567.00	701.00	145.00	118.00
1898	0.00	453.00	654.00	642.00	102.00	45.00
1545	0.00	278.00	509.00	576.00	135.00	48.00
1034	0.00	201.00	329.00	385.00	79.00	41.00
1945	0.00	301.00	649.00	721.00	156.00	110.00
1742	0.00	300.00	598.00	621.00	143.00	77.00
1732	0.00	280.00	543.00	689.00	113.00	107.00
1698	0.00	273.00	632.00	601.00	142.00	51.00
1778	0.00	256.00	653.00	672.00	142.00	55.00
1350	0.00	201.00	498.00	498.00	97.00	56.00
1534	0.00	254.00	560.00	532.00	153.00	35.00
1509	0.00	231.00	583.00	560.00	100.00	35.00

Table A.3.: Distribution in grams for each grain size interval for Vassfjellet 4/8

A. Appendix

	Distribution [%]					
	>11.2 [mm]	8-11.2 [mm]	6.3-8 [mm]	5-6.3 [mm]	4-5 [mm]	<4 [mm]
Average	0.00	16.62	35.00	37.09	7.62	3.63
Relative standard deviation	0.00	0.15	0.062	0.05	0.15	0.38
Sample mass [g]						
1832	0.00	14.52	35.86	37.77	8.30	3.55
1983	0.00	14.42	39.74	32.83	7.97	4.79
1680	0.00	18.69	36.61	35.18	6.90	2.38
1778	0.00	14.51	33.63	41.28	8.27	2.25
1612	0.00	22.70	37.66	33.13	6.08	1.80
1666	0.00	18.67	34.09	37.09	6.60	3.36
1615	0.00	15.48	32.38	40.37	7.74	3.72
1576	0.00	17.45	35.53	37.69	6.54	2.79
1821	0.00	18.67	33.22	37.78	7.63	2.69
1746	0.00	14.83	33.33	38.32	8.13	4.81
1684	0.00	17.40	38.60	35.93	5.82	1.90
1568	0.00	16.71	32.91	37.44	7.33	5.36
1842	0.00	13.90	34.20	39.03	8.85	3.75
1670	0.00	16.77	34.25	37.78	8.32	2.81
1596	0.00	15.23	35.09	34.71	8.96	6.20
1656	0.00	17.33	35.81	39.43	5.56	1.93
1594	0.00	14.49	35.63	37.14	9.10	3.83
1756	0.00	12.70	32.29	39.92	8.26	6.72
1898	0.00	23.87	34.46	33.83	5.37	2.37
1545	0.00	17.99	32.94	37.28	8.74	3.11
1034	0.00	19.44	31.82	37.23	7.64	3.97
1945	0.00	15.48	33.37	37.07	8.02	5.66
1742	0.00	17.22	34.33	35.65	8.21	4.42
1732	0.00	16.17	31.35	39.78	6.52	6.18
1698	0.00	16.08	37.22	35.39	8.36	3.00
1778	0.00	14.40	36.73	37.80	7.99	3.09
1350	0.00	14.89	36.89	36.89	7.19	4.15
1534	0.00	16.56	36.51	34.68	9.97	2.28
1509	0.00	15.31	38.63	37.11	6.63	2.32

Table A.4.: Distribution in percent of mass for each grain size interval for Vassfjellet 4/8

A.2. The Thesis as an Academic Journal Article

Begins on the next page.

Construction of a Functional 1:5 Scaled Ballasted Railway Track

A. Wigaard¹

¹Department of Civil and Environmental Engineering, NTNU, Norway

Abstract

This paper concerns constructing and validating a 1:5 scaled ballasted railway track. The construction is cost-effective and time-efficient by employing commercially available components, albeit compromising some properties and realism. The constructed model, named the Wigaard track (TWT), is subjected to vertical load to measure the track's vertical deflection. Results show deviations from theoretical predictions, highlighting the need for improved scaling functions and load distribution analysis. TWT is an initial step towards developing a versatile representation of full-scale ballasted railways, aiming to provide valuable data for future research and analysis.

Keywords: scaled model, laboratory model, superstructure, vertical deflection, test apparatus, ballasted track.

1 Introduction

Rail transportation is safe and environmentally friendly, but Norway's rail network outside cities is limited due to high costs. Improving track design and construction can optimize efficiency and cost-effectiveness. Scientific research, including physical model experimentation, can enhance track safety and maintenance. A functional, scaled, ballasted railway track for laboratory experimentation will be developed as part of a master's thesis at NTNU, with essential findings summarized in this paper. The complete master's thesis is available at NTNU open.

1.1 Motivation

Scaled ballasted railway track is a viable and versatile scaled apparatus for scientific research [1]. Full-scale railway tests are rare, expensive, and often inaccessible, limiting innovation. Scaled systems can provide useful data but cannot perfectly represent the track's behavior. This research aims to create the best possible scaled representation of a ballasted railway track. Such a representation can produce meaningful results in different loading situations. Model testing will merely waste time and money if theory alone can predict the results. Additionally, practical testing will have no advantages if the experiment is too complex, and the scaled model is not expected to represent full-scale behavior realistically [2]. These two criteria establish an explicit range for the usage of the scaled models.

The smaller scale has benefits such as easier operation, quicker parameter changes, and lower costs. Laboratory testing allows for controlled conditions and isolated parameter testing. The reduction in experiments' loading magnitude has previously proved to be the most cost-beneficial aspect of small-scale research [3].

The scaled model will be simple, affordable, and operable to meet the limited time-frame of the research. Common and commercially available materials will be used to build the track, compromising its performance and similarity but creating a lower threshold for future similar projects.

1.2 Contribution

The master's thesis's main contribution is to provide NTNU with an operable and affordable apparatus for practical railway research and experience on the topic.

A literature search was conducted in the author's specialization project [4]. The scarcity of scaled ballasted railway models and the often unsatisfactory description of design and construction is a knowledge gap this thesis attempts to fill.

1.3 Objective

This research is motivated by eventually creating the best possible representation of a railway track on a manageable scale. However, in this iteration of the scaled model, the objective is to:

Construct the best possible functional 1:5 railway track from easily accessible material

The secondary objective is to survey the similarity between the scaled model and full-sized railways. Conclusions on similarity will be made by validation testing on the assembled model.

1.4 Research Questions

- How does one build the best possible 1:5 scaled ballasted railway track with commercially accessible material?
- How similar to a full-sized railway track will the scaled track behave under static vertical load?
- What design compromises in the scaled track significantly impact its similarity to a full-scale track?

1.5 Scope

The scaled model built in this research is approximately geometrically similar to a ballasted railway track's superstructure. In the research, a 1:5 scaled ballasted railway track will be built. The track will be tangent and 2.5 meters long. The scaled model shall consist exclusively of rails, sleepers, a fastening system, and ballast resting on a concrete floor. A vertical load test will be performed to analyze the scaled model's similarity and performance. Only commercially available material will be used, and there will be no extensive processing of the prefabricated components.

2 Theory

The theory discusses an overview of scaling theory, how relevant track forces affect a railway, and how a loading situation is attempted to be replicated in scale. BaneNOR's superstructure class d is used as a reference for comparison.

The scaled model will be designed approximately geometrically similar to superstructure class d. A perfectly geometrically similar model in scale will have significant distortions in properties. The most prominent distortions to this research's validation testing will be discussed in Section 3.1.

2.1 Scaling and Similitude

A scaled model represents a full-size structure reduced in size to perform experiments more efficiently. Rayleigh first discussed small-scale modeling interpreted through the principle of similitude and dimensional analysis in 1915 [5]. It has since been further reviewed and modified by Langhaar [2], among others. Laws of similitude must be used when interpreting test results [3]. However, finding a numerical coefficient through the principles of similarity is impossible. It will require deep calculation or experimentation [5]. For the scaled track, results from validation testing will be used to derive a scaling coefficient or function, accurately relating input and output parameters between the full-size track and the scaled model.

Understanding the impact of small scale on materials and structures is crucial for accurate model studies. Smaller components typically have a lower probability of flaws, thus greater relative strength [3, 6]. Furthermore, geometrically similar structures will be affected by gravity linear to their mass, which is downscaled cubically, making the lighter structure relatively less affected by its specific weight and thus stronger [5]. Results from one scale cannot be directly compared to another [6].

The uncertainties associated with scaling are one reason scaled railway tracks are scarce. For an intricate structure like a railway superstructure, complete similitude is impossible. Instead, partial similarity is obtained by establishing geometrical similarity as a scaling condition. To correctly interpret data from scaled model testing, one must determine proper scaling factors, establish necessary conditions that relate the response behavior of the scaled system to the full-sized system, and understand how much the scale affects the accuracy of model behavior [7].

2.2 Theoretical Relation Between Static Vertical Force and Vertical Deflection

This research will conduct a static vertical loading experiment on the scaled model, where vertical deflection is measured. Vertical loading capacity is an essential measure of a track's quality and is chosen because the required set-up for applying a static vertical force is affordable and manageable. A criterion for the chosen validation test is that it must have a correct answer to strive for, and the relation between deflection and vertical load on a full-scale track can be calculated using theory.

The validation test represents one nominal axle load exerted on a superstructure of BaneNOR's class d, which is 22.5 tonnes. Theoretically, the load should be reduced proportionately to the square of the geometrical scale factor [3]. For the 1:5 scaled system, a 22.5 tonnes axle load is best represented by 4.4 kN static vertical force on each rail.

2.2.1 Mathematical Formulas and Relevant Track Properties

Deflection, bending moment, and bending stress limit a railway's ability to handle large vertical loads. These parameters can be calculated for a full-sized track by treating the rails as a continuously supported beam. The theory is shown in equation 1-3[8].

$$y = \frac{Q}{2kL} \quad (1) \quad M = \frac{QL}{4} \quad (2) \quad \sigma = \frac{M}{W} \quad (3)$$

- y = Deflection, [m]:
- σ = Bending stress, [N/mm²]:
- M = Bending moment, [kNm]:

- Q = Wheel-load, [kN]
- k = foundation coefficient (track modulus), [N/m²]
- L = characteristic length, [m]
- W = second moment of area, [m³]

Track modulus, k , is the elastic support under the rails, depending on ballast, foundation, and sleepers. Characteristic length, L , is the length of the rail affected by deflection and depends on the rail profile and foundation. The second moment of inertia, W , is the moment of inertia, I , divided by the vertical distance, z , from rail-foot to the cross-section's centroid.

$$k = \frac{C \cdot A_{rs}}{s} \quad (4) \quad L = \sqrt[4]{\frac{4EI}{k}} \quad (5) \quad W = \frac{I_x}{z} \quad (6)$$

- C = foundation modulus, [N/m³]
- A_{sl} = area of the sleeper, [m²]
- s = sleeper distance, [m]
- E = elastic modulus, [N/m²]
- I = moment of inertia, [m⁴]
- z = vertical distance from rail-foot to the cross-section's centroid [mm]

The theory for predicting vertical deflection in a full-scale system may not apply to a 1:5 scale due to parameter distortions. A scaling function will be created to analyze the difference.

3 Methodology

3.1 Material Choices and Distorted Properties

3.1.1 T-Profile Steel Bars as Down-Scaled Rails

T-profile steel bars will be used as rails on the scaled track. Initially, a 35 mm x 35 mm T-section was preferred, but issues with steel distributors led to the purchase of a 6-meter, 40 mm x 40 mm T-section steel bar with a thickness of 5 mm. The steel's quality is S235J. The scaled rails bending stiffness is distorted due to the scaling. Using equation 7, the scaled rail's moment of inertia is estimated to be 5.56 cm⁴. The full-sized 60E1 profile's moment of inertia is 3038.3 cm⁴ [9]. Equation 7 calculates the moment of inertia over the scaled rail's lateral axis, I_y , where the T-profile is interpreted as two rectangles with height, h_i and width, b_i :

$$I_y = \sum_{i=1}^2 \left(\frac{1}{12} \cdot b_i h_i^3 + A_i \cdot e_i^2 \right) \quad (7)$$

The moment of inertia is down-scaled cubically with a cross section's height. This problem is inevitable when down-scaling. Additionally, the T-section geometry is less ideal than a rail with a railhead. There is less surface area far from the centroid, which drastically reduces e_2 , contributing squared to the total moment of inertia. Stresses applied to the scaled rails must never cause permanent deformations. Rail bending stiffness greatly influences the track's bearing capacity, rail bending stress, rail stiffness, and rail deflection [8].

The T-profile was cut into two 2.5-meter rails.

3.1.2 Scaled Sleepers Made of a Square Steel Pipe

The sleepers are made of a hollow steel pipe with a cross-section of 40 mm · 60 mm and 3 mm thick walls. The steel is of quality S355J2H. The pipe's width and height are approximately 1/5 of the JBV60's width and height. The pipe will be cut into parts with a length of 480mm, and this length is chosen to get the surface area that allows theoretical deflection and rail stress to be equal to a full-size railway simultaneously.

The relative difference in weight and material choice influences lateral resistance. Previous research found that the lateral resistance is expected to be 1/125 of a full-size sleeper [10, 11], and steel sleepers perform insufficient in dynamic lateral resistance[12]. The sleepers will be filled with concrete to increase the mass and geometrical similarity. The sleepers have a mass of 4.5 kg. Comparatively, one JBV60 sleeper weighs 285 kg [9].

Before filling the hollow profile, four 17mm hexagonal holes were made to insert coupling nuts for the fastening. The coupling nuts were 40mm, protruding slightly on one side of the sleeper. The protruding was lower than the thickness of the rail foot and proved helpful when aligning the rails at constant track gauge.

3.1.3 Fastening System

The fastening system will be simplified, justified by a relative reduction in loading magnitude and the absence of electric current, rendering insulation excessive. The primary purpose of a fastening system is to hold the rails in place at a constant track gauge. The scaled fastening system achieves this by clamping the rail to the sleeper with a force 1/5 of the requirement of full-scale fastening systems for superstructure class d, which is 18 kN on each side of the rail $\pm 30\%$ [9]. The scaled fasteners are one square washer on each side of the rail, an accompanying coupling nut inside the scaled sleeper, and a bolt strong enough to perform the decided clamping force, 3.6 kN. The scaled track gauge is 287mm, 1/5 of the full-scale track gauge of 1435 mm. The square discs are 40 x 40 mm with a 12mm diameter hole in the center, and the

bolts have a diameter of 10 mm with an 8mm head. The dimensions were chosen to perform a clamping force of 3.6 kN per bolt based on the guidance of experienced laboratory engineers.



Figure 1: Scaled sleepers



Figure 2: Fastening system and rail

3.1.4 Scaled Ballast Material

Previous research finds negligible differences in scaled grain's aspect ratio and concludes that scaled ballast material should have gradation parallel to the full-size material it represents [13, 14]. Therefore, the scaled model will use grain distribution parallel with BaneNOR's requirements [15, 16], down-scaled by 1/5.

Scaled ballast material production is the scaled track's most comprehensive individual component. The scaled requirements for grain distribution differ from the available standard sieve sizes. Sieving analysis reveals that scaled ballast material cannot be produced by taking crushed stone directly from the purchased pallet frames. Therefore, the material is sieved, sorted, and put together to an acceptable grain distribution, shown in Figure 3.

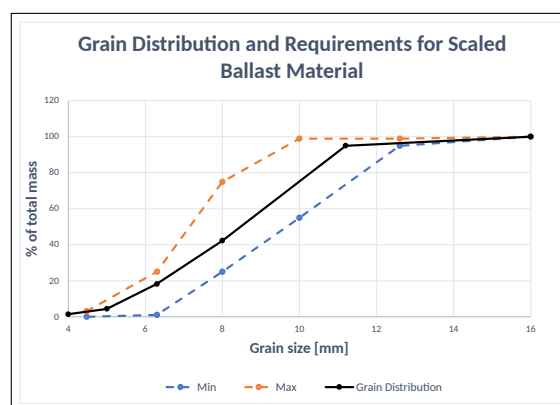


Figure 3: Distribution curve for scaled ballast material

The crushed rock used was obtained from the Vassfjellet quarry and is of excellent quality. Los-Angeles value, Micro-Deval coefficient, flakiness index, and shape index

are all within full-scale requirements by substantial margin. The layer's cross-section is linearly down-scaled with a factor of 1/5 from BaneNOR's standard ballast cross-section for a single tangent track. A height of 800mm on a stiff subgrade is required on real railways, corresponding to 160mm in scale.

3.2 Construction of the Scaled Track

The ballast material was laid on a rug and shaped to the correct trapezoidal shape. Ballast height and shape were controlled by long metal bars held correctly by custom wooden supports and markings on the rug.

The sleepers were aligned with two measuring tapes at predetermined longitudinal coordinates, locked together with the rails, and lifted onto the ballast layer. Next, the structure was jogged deeper into the ballast. After ensuring that the height from the floor to the top of the sleepers was 160 mm and that the track was level longitudinally and laterally, the rails were removed. The sleepers were then buried in additional ballast material, fully integrating the sleepers. Finally, the rails were fastened again, and the model was completed.



Figure 4: Sleepers connected by rails Figure 5: Structure lifted onto the ballast



Figure 6: Integrating the sleepers Figure 7: Finalized scaled model

3.3 Set-Up for Validation Testing

A set-up capable of delivering desired loading magnitude must be created to perform vertical load tests on the scaled model. Once completed, it will measure the foundation coefficient, C , before tests are conducted on the scaled track. When a C -value is estimated, the validation tests on the scaled track proceeds.

3.3.1 Vertical Load Set-Up

The set-up must be capable of delivering 8.8 kN of vertical load. A hydraulic jack was chosen, and a frame spanning the lateral direction of the track was built to hold the jack. The frame must have negligible vertical deflection under relevant loading magnitude, meaning the beam over the track must be robust. The best option was a full-scale rail, held down by four nuts on four threaded rods fastened to the floor. Two hollow metal posts were placed around the threaded rods to stiffen the frame.



Figure 8: The frame spanning the scaled model



Figure 9: The rail as a beam, threaded rods, and fastening nuts

A dial gauge and a calibrated load cell were used for measurements. Three different testing positions were prepared. One testing position was at the longitudinal center of the scaled track, while two others were placed on the north and south sides, equally distant from the center and the track's ends. The positions were named N, C, and S, as shown in Figure 10-12.



Figure 10: Test position N



Figure 11: Test position C



Figure 12: Test position S

Data points consisting of vertical force on each rail, Q , and deflection, y , were plotted for both tests. These data points' rate of increase and linearity are the interesting parameters.

3.3.2 Determining Foundation Modulus for the Scaled Model

The foundation modulus will be measured with two unique steel plates as contact areas to the ballast layer at the three different test positions, six tests total. The plates are small to ensure the entire area is in contact with the ballast. Data points are plotted when both load and deflection have a steady value to read.

3.3.3 Static Vertical Load Test

Three different sleeper distances are tested to reveal if a change in sleeper distance has the same effect on vertical deflection as the theory suggests. The sleeper distances tested are 111mm, 153mm, and 222mm. A rigid steel cylinder with a diameter of 45mm is used to represent a wheelset. The cylinder is assumed to have negligible vertical deflection during testing. It was attached to a jack with a magnetic base and placed in the center of the track. A small platform was fastened perpendicular to the loading direction to measure the deflection.



Figure 13: Vertical load test



Figure 14: Measurement of C-value

4 Results

4.1 The Wigaard Track (TWT)

The main result of the research is the finished scaled model, named the Wigaard track. The physical model is constructed and can be further validated, improved, and potentially used for functional laboratory experimentation. TWT represents a tangent ballasted railway track on a scale of 1:5.



Figure 15: The Wigaard track, a 1:5 scaled ballasted railway track

4.2 Foundation Coefficient for The Wigaard Track

Table 1 shows the average foundation coefficient of six loading tests on the scaled model. The tests varied three different positions and two different steel plates. Normal

full-scale conditions are also listed for comparison.

C-value [N/mm ³]	Terrain
< 0.05	Soft sub-grade, I.e marches or
0.05-0.15	Soft to firm clay
>0.3	Solid rock or concrete
0.0478	The scaled ballast layer on concrete

Table 1: Values for foundation modulus on full-scale ballasted tracks, and the scaled track's average measured C-value

The measured value could not have been foreguessed, and the research needed an independent estimation before the static vertical load test was conducted. Without a predetermined C-value, any linear results would align with a costume C-value, which does not reveal how applicable the full-scale theory is in the scaled system.

4.3 Results from Static Vertical Load Test

The load chosen to represent the nominal axle load, 4.4 kN, is used in Excel to calculate the expected deflection, bending stress, and bending moment in the scaled system, presented in Table 2. Vertical load, Q, and deflection, y, have a linear relationship. Figure 16 - 19 shows the results plotted with the expected linear trend lines.

Q ₀ = 4.4 kN								
s[mm]								
111	153	222	111	153	222	111	153	222
M [Nm]			σ [N/mm ²]			y [mm]		
272.43	295.01	323.98	57.97	62.77	68.93	0.7156	0.9087	1.2035

Table 2: Theoretical bending stress, bending moment, and deflection for the scaled loading situation

Four points are plotted for every loading to check the linearity. The points were evenly spread out from Q=0 to Q=4.4 kN, where the recordings showed clear and steady readings on both the load cell's display and the dial gauge. Unfortunately, some data was invalid on the two last tests, the center and south tests on sleeper distance 153 mm. The reason and implications will be discussed in section 5.1.

The data shows a linear trend between vertical deflection and vertical load. The data points for sleeper distances 111 mm, 153 mm, and 222 mm have corresponding Pearson correlation coefficients of 0.953, 0.997, and 0.948. The rate of increase of a linear regression line for each data set is 0.3082 m/N, 0.4006 m/N, and 0.4007 m/N for decreasing sleeper distance. In other words, changing sleeper distance has the expected effect, but only marginally between s=153 mm and s=111 mm. The average deviation from theory is calculated for each data point as the difference between the

measured and calculated values at an equal vertical load. The average deviation from theory was 66.81%, 51.85%, and 31.39% for sleeper distances 111 mm, 153 mm, and 222 mm respectively.

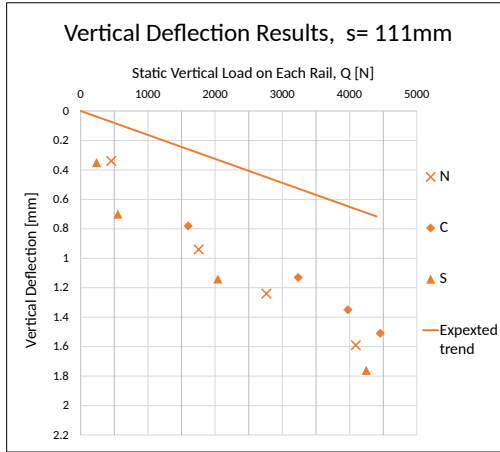


Figure 16: Data plot for s=111 mm

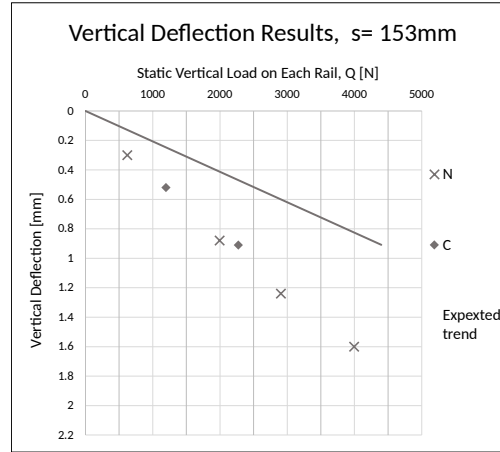


Figure 17: Data plot for s=153 mm

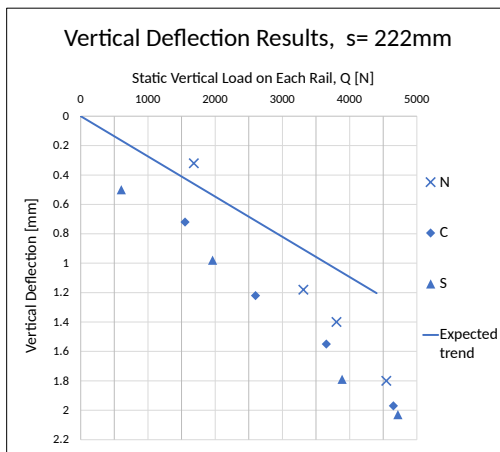


Figure 18: Data plot for s=222 mm

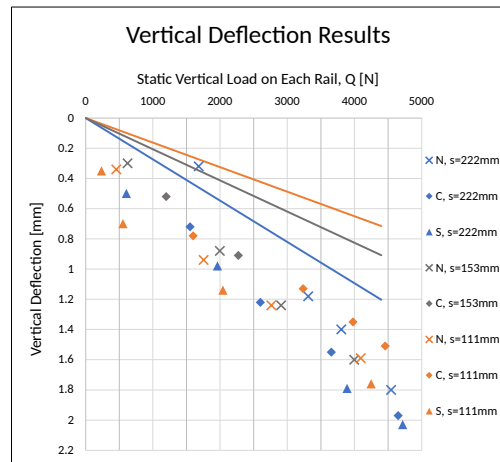


Figure 19: Data plot for every test

4.4 Suggested Scaling Function for Vertical Deflection

This result gives an improved mathematical formula for the relation between static vertical force and vertical deflection in the scaled system. The existing formula for full-scale tracks is used and expanded on with a function of sleeper distance. The function exclusively applies to TWT and is added to the existing formula. The function is $W(s)$, where s is the dimensionless input of the sleeper distance's meter value. $W(s)$ is a suggested function rather than a scaling law due to the small dataset. Figure 20 shows the adjusted theoretical deflection for each sleeper distance along the data from the tests.

$$W(s) = 0.823 \cdot s^{-0.494} \quad (8)$$

$$y = \frac{Q}{2kL} \cdot 0.823 \cdot s^{-0.494} \quad (9)$$

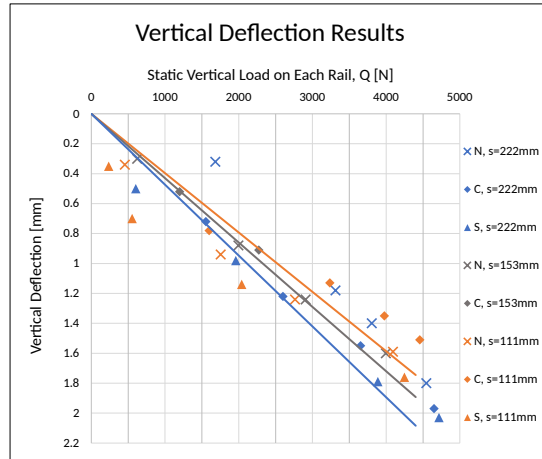


Figure 20: New expected results using suggested scaling function in the results plot

The Wigaard function works best for the sleeper distance of 153 mm and must never be used for sleeper distances over 222 mm or under 111 mm. It gives a 19.03% average percent deviation for $s=111$ mm, -18.5% for $s=222$, and -0.36% for $s=153$ mm. $W(s)$ is dimensionless and can be calculated as a scaling coefficient if the sleeper distance is constant. For example, the sleeper distance closest to $1/5$ of 600mm using the whole track and a whole number of sleepers is 128 mm. A scaling coefficient of 2.28 can be used instead of the formula for this constant sleeper distance.

5 Discussion

5.1 Damaged Threads on the Loading Set-Up Causing Invalid Data

During validation testing, two of the nuts slipped and caused two threaded rods to wear out. As a result, the frame had significant vertical deflection during tests. The last test was conducted, but the data was useless due to the frame's lack of rigidity. It is uncertain whether the set-up was less capable than presumed or if the nuts were tightened unevenly. The incident made a loud sound caught by the recording, making it possible to distinguish valid and invalid data. The valid data obtained from the affected sleeper distance followed the expected deflection. Therefore it was deemed unnecessary to finish testing. The data from tests sleeper distance 153mm is nevertheless more uncertain than the other.

5.2 Properties of TWT

TWT has several adjustable features, which can be altered to best fit future research. Two of the most manageable parameters to change include ballast height and sleeper distance. One can shorten sleepers to get a smaller surface area supporting the rails. Reduction of sleeper area increases deflection more than bending stress, making it possible to simultaneously get both parameters equal to a full-size railway under any given axle load. Naturally, there is no way back to the original sleeper length, so caution is advised. The track is 2.5 meters long and takes up approximately three m² of floor space when assembled. The ballast can fit on one pallet with three pallet frames and is about 700 kg of mass, which makes up most of the total model's weight. The price of TWT is approximately 3600 NOK, excluding the loading set-up, loading equipment, and transportation costs.

5.3 The Scaled Track's Loading Distribution and Characteristic Length

The results show that sleeper distance has a less prominent effect than in theory. This difference between theory and measurements is indisputable and significant for all three sleeper distances. The reason why more sleepers do not increase the track resistance to vertical deflection can be poor load distribution. In other words, the characteristic length, i.e., the length of rail affected by vertical deflection, is shorter than the theory suggests. Consequently, the load is distributed over fewer sleepers, resulting in relatively higher vertical deflection.

Various factors can cause weak load distribution on TWT. The characteristic length of the sleeper distance should span multiple sleepers for proper load distribution. A shorter characteristic length may result in inefficient load distribution. The sleeper's shape, material, or surface area reduction due to scaling may impede load distribution. Weak bending stiffness of the rails can cause high vertical deflection, and it can have an effect on the applicability of mathematical formulas. The rail bending stiffness distortion is TWT's most prominent parameter distortion.

5.4 Further Work

Further work on the Wigaard track is the only way to produce a multi-purpose scaled model for laboratory experimentation that can be used in railway technology innovation. Such a model would be a valuable asset to the academic community at NTNU and the railway research community nationwide. Improvements and further work on TWT can be replacing the scaled rails, replacing the scaled sleepers, dynamic load validation test, and researching the model inside the snow laboratory. These suggestions are only for inspiration. Future researchers must be imaginative and choose research suitable for their motivation and competence.

6 Conclusions

This section presents concise answers to the research question and an assessment of the objective based on the results and discussions. The conclusion of this research is:

- The best possible 1:5 scaled ballasted railway track is built over several iterations. It is necessary to research available materials and purchase those with dimensions closest to 1/5 of a full-scale track. The next step is to assemble and test the behavior of the scaled track. Afterward, the behavior of the scaled track is compared with the desired behavior, any distortions that cause dissimilarities are identified, and improvements are suggested. This process is repeated until the track is expected to produce meaningful results that cannot be predicted solely through theory.
- The scaled track has relatively high vertical deflection under static vertical load. However, a full-scale nominal axle load situation can be accurately represented in the scaled system with a sleeper distance of 128 mm and a load down-scaled by 1/25. Furthermore, a scaling function can be used to predict vertical deflection on the track. For a sleeper distance of 128 mm, vertical deflection can be calculated with the full-scale mathematical formula multiplied with a numerical coefficient of 2.27.
- The scaled track does not distribute vertical force as well as a full-scale track. Amongst the relevant track properties for this research, the bending stiffness of the scaled rail is distorted most in the scaling. The distortion is caused by both the reduction in scale and the compromise made for commercial availability and likely has a profound effect on the rail's ability to distribute loads.

The objective of the research is to construct the best possible scaled track with commercially available material. There are better imaginable scaled representations of a ballasted railway track than this attempt. However, it is the best possible first iteration of a functional scaled ballasted railway track, considering the author's limited time frame, previous experience, and the commercial availability condition. The research is only the first step in creating a versatile representation of a full-scale ballasted railway track that can produce meaningful data in multiple new loading situations. This ultimate goal is still further down the road and will require more iterations of the model, cooperation, and sharing of experiences.

Acknowledgements

The author thanks Albert Lau for expert guidance on the railway theory and Bent Lervik, Tage Westrum, and Torbjørn Nerland for support, guidance, and help in practical construction, material ordering, material processing, and laboratory work. Finally, a big thanks to Konnekt for the necessary monetary funding.

References

- [1] Vahid Najafi Moghaddam Gilani, Mohammad Habibzadeh, Seyed Mohsen Hosseinian, and Reza Salehfard. A review of railway track laboratory tests with various scales for better decision-making about more efficient apparatus using topsis analysis. *Advances in Civil Engineering*, 2022:9374808, 2022.
- [2] H.L. Langhaar. *Dimensional Analysis and Theory of Models*. John Wiley & Sons, 1951.
- [3] Harry G Harris. *Structural modeling and experimental techniques*. CRC Press, Boca Raton, Fla, 2nd ed. edition, 1999.
- [4] A. Wigaard. Surveying design and scaling strategy of a 1:5 scaled ballasted railway track for functional laboratory experimentation, des 2022. Specialization project, not available online.
- [5] Rayleigh. The principle of similitude. *Nature*, 95(2368):66–68, 1915.
- [6] Aksana Jihad Mohammed, Naseer Babangida Muazu, Baba Shehu Waziri, and Taghadosi Ahmad. Models and size effects: A review. *IOSR Journal of Mechanical and Civil Engineering*, 12:54–59, 2015.
- [7] Shadi Balawi, Owais Shahid, and Mohammad Al Mulla. Similitude and scaling laws - static and dynamic behaviour beams and plates. *Procedia Engineering*, 114:330–337, 2015.
- [8] A. Lau. *Compendium TBA4225 Railway Engineering, Basic course*. NTNU, 2022.
- [9] BaneNOR. Teknisk regelverk/ overbygning/ prosjektering/ sporkonstruksjoner/, [updated 2022; cited 2022 okt 18].
- [10] Yohei Koike, Takahisa Nakamura, Kimitoshi Hayano, and Yoshitsugu Momoya. Numerical method for evaluating the lateral resistance of sleepers in ballasted tracks. *Soils and Foundations*, 54(3):502–514, 2014.
- [11] H Tomita, Kimitoshi Hayano, and P Anh. Effects of model scale on lateral resistance characteristic of sleepers in railway ballasted tracks. In *Bearing Capacity of Roads, Railways and Airfields*, pages 2047–2054, 06 2017.
- [12] Morteza Esmaeili, Saeed Majidi-Parast, and Ahmad Hosseini. Comparison of dynamic lateral resistance of railway concrete, wooden and steel sleepers subjected to impact loading. *Road Materials and Pavement Design*, pages 1–28, 05 2018.
- [13] Adam F Sevi. *Physical modeling of railroad ballast using the parallel gradation scaling technique within the cyclical triaxial framework*. Missouri University of Science and Technology, 2008.
- [14] Louis Le Pen, William Powrie, Antonis Zervos, Sharif Ahmed, and Sinthuja Aingaran. Dependence of shape on particle size for a crushed rock railway ballast. *Granular Matter*, 15, 12 2013.
- [15] BaneNOR. Tekniske spesifikasjoner/ overbygning/ ballast, [updated 2015; cited 2022 Okt 22].
- [16] European committee for standardization. Aggregates for railway ballast. NS-EN 13450, 2002.